
Data-adaptive exposure thresholds for the Horvitz-Thompson estimator of the Average Treatment Effect in experiments with network interference

Vydhourie Thiyageswaran
Department of Statistics
University of Washington

Tyler McCormick
Department of Statistics
University of Washington

Jennifer Brennan
Google Research

Abstract

Randomized controlled trials often suffer from interference, a violation of the Stable Unit Treatment Values Assumption (SUTVA) in which a unit's treatment assignment affects the outcomes of its neighbors. This interference causes bias in naive estimators of the average treatment effect (ATE). A popular method to achieve unbiasedness is to pair the Horvitz-Thompson estimator of the ATE with a known exposure mapping: a function that identifies which units in a given randomization are not subject to interference. For example, an exposure mapping can specify that any unit with at least h -fraction of its neighbors having the same treatment status does not experience interference. However, this threshold h is difficult to elicit from domain experts, and a misspecified threshold can induce bias. In this work, we propose a data-adaptive method to select the " h "-fraction threshold that minimizes the mean squared error of the Horvitz-Thompson estimator. Our method estimates the bias and variance of the Horvitz-Thompson estimator under different thresholds using a linear dose-response model of the potential outcomes. We present simulations illustrating that our method improves upon non-adaptive choices of the threshold. We further illustrate the performance of our estimator by running experiments on a publicly-available Amazon product similarity graph. Furthermore, we demonstrate that our method is robust to deviations from the linear potential outcomes model.

1 Introduction

Under network interference, where the Stable Unit Treatment Values Assumption (SUTVA) is violated, estimating average treatment effects incorporating direct effects (impact of the treatment on the respondent's outcome) and indirect effects (impact of treated peers on the respondent's outcome) is a central problem in learning causal effects. We study the setting of randomized controlled trials. For example, estimating the adoption of a new idea through random assignment of people to advertisements is complicated by the dissemination of information through social interactions. In settings where user behavior informs a prediction algorithm, the behavior of other users creates spillovers through their impact on the prediction algorithm. As such discrete interactions can be modeled through network interference models, the problem of estimating average treatment effects under network interference becomes a ubiquitous one.

A major challenge arises from the lack of knowledge of the exact interference structure that contributes to the indirect effect. For some treatments, having treated peers might have very little impact (e.g. a drug for a noncommunicable disease that's only available as part of a clinical trial), whereas for others the impact could be extremely large (e.g. vaccines). *Exposure maps* classify individuals into groups with similar contact patterns with treated peers.

One simple form of exposure map classifies individuals as indirectly exposed if more than some fixed fraction h of their network is treated, meaning that the researcher expects contact with a smaller fraction than h to have no impact on the outcome and a fraction larger than h to have a substantial, but relatively consistent impact as the fraction increases above the threshold. Our setting corresponds to what Centola and Macy [2007] refer to as *contested contagion*. That is, settings where *both* treated and untreated peers influence an individual’s outcome, but in different directions, and the size of the respondents’ network also matters. Centola and Macy [2007] give an example of cleaning litter from a beach—a person might be willing to pick up litter alone if 10 people use the beach, but the task would seem futile without a group of civically-minded individuals if 1,000 people use the beach. This conception of exposure is particularly salient in studying the adoption of technology, particularly in settings where the technology becomes more useful as more members of the network adopt it, known as the “threshold of adoption” [Acemoglu et al., 2011, Reich, 2016]. Adopting a messenger app, for example, becomes more appealing as a larger fraction of social contacts also use the app.

Given a known h -fractional exposure mapping, the Horvitz-Thompson estimator under this criterion is commonly used as an unbiased estimator of the average treatment effect. Without domain knowledge of the interference structure, however, an estimator with fixed treatment exposure conditions for this estimand will be high in either bias or variance. One could, for example, resort to using the Horvitz-Thompson estimator at extreme h s for unbiasedness, such as when the unit in question, and *all* its neighbors are treated. However, this incurs the cost of a large variance, as the estimator scales inversely with the probability of the unit and all its neighbors being treated. This probability can be very small for high-degree nodes, particularly, in dense graphs and when treatment fractions are small. Choosing a small threshold, however, means that many individuals who are in reality not impacted indirectly by the treatment will be counted amongst the indirectly exposed, biasing effect estimates. This motivates the study of mean-squared-error (MSE)-minimizing exposure threshold selection to combine with existing estimators.

Our contribution to this setting is to propose a simple, data-dependent approach to estimating the average treatment effect optimally in terms of the MSE. We compute an approximate rate of change of bias and variance with respect to the threshold to inform the MSE-optimal threshold for the Horvitz-Thompson estimator. In particular, we propose using linear regression for an approximate bias-rate of change measure as a simple and intuitive approach. Additionally, this study allows us to understand graph structures under which this approximation is more precise.

1.1 Related Works

The exposure mapping framework is a common strategy for quantifying spillovers. In Aronow and Samii [2017], Ugander et al. [2013], Sussman and Airoldi [2017], Hardy et al. [2019], and Auerbach and Tabord-Meehan [2021], the authors expounded upon different exposure mappings, and estimation under these settings. Eckles et al. [2017], Toulis and Kao [2013] assume a (weighted) fraction of treated neighbors in characterizing the exposure. We work under a similar setting. Other common assumptions include exposures described by the raw count numbers of the treated/control neighbors Ugander et al. [2013]. In Basse and Airoldi [2018], Cai et al. [2015], a (known) generalized linear form of network effects on neighborhood treatments was assumed. We do not assume this. Related to our work, in Zhu et al. [2024], the authors fit functionals on the treatment assignment and exposure.

For off-policy evaluation in reinforcement learning, Su et al. [2020] investigate adaptive MSE-optimal kernel bandwidth selection (a widely studied problem, see for example, Fan and Gijbels [1992], Ruppert [1997] Kallus and Zhou [2018]) using Lepski’s method Goldenshluger and Lepski [2011]. To the best of our knowledge, a reframing of our problem in terms of optimal bandwidth selection A.3 has not been studied in the average treatment effect estimation under network interference setting. The authors of Belloni et al. [2022] have a different, but related, goal of estimating the direct effect under network interference. Their approach was to first estimate interference structure by estimating the m_i -hop influence (beyond the immediate graph neighborhood), or exposure radius under assumptions of additivity of the main effects in the potential outcome model.

1.2 Notation.

We use h to denote the threshold for “treatment exposure”, and $1 - h$ for “control exposure.” Therefore, for larger h , i.e. h closer to one, we have a more restrictive setting, where only the subset of treated

(resp. control) units with most of their neighbors treated (resp. control) are counted as treatment (resp. control) exposed. For smaller h , i.e. h close to zero, we have a less restrictive setting, as a larger subset of treated (resp. control) units satisfy the threshold condition. Throughout the paper we use d_i for the degree of node i , and d when the graph is regular.

2 Setup

We consider a fractional exposure mapping. That is, for any treatment assignment vector $\mathbf{Z} \in \{0, 1\}^n$, the effective influence of the graph's treatment assignment on the outcome of node i is equivalent to the influence of fractional treatment assignments in the neighborhood of node i . This reduces our potential outcome model that so that it takes the following form:

$$y_i(\mathbf{Z}) = y_i(z_i, e_i) = \alpha + g(z_i) + f(e_i) + \epsilon_i \equiv \alpha + \psi(z_i, e_i) + \epsilon_i, \quad (1)$$

where $z_i \in \{0, 1\}$ is the treatment assignment of unit i , $e_i \in [0, 1]$ is the fraction of treated neighbors of unit i (not including i itself), and ϵ_i are independent (and independent of (z_i, e_i)) sub-gaussian noise with mean zero, and variance σ^2 . We denote by Y_i the observations under this potential outcome model.

We are interested in estimating the average treatment effect (ATE)

$$\tau = \frac{1}{n} \sum_{i=1}^n Y_i(1, 1) - \frac{1}{n} \sum_{i=1}^n Y_i(0, 0), \quad (2)$$

though we could, more generally, take any difference between exposure categories. We will consider the Horvitz-Thompson estimator for a given exposure threshold h :

$$\hat{\tau}_h = \frac{1}{n} \sum_{i=1}^n \frac{\mathbf{1}\{z_i = 1, e_i \geq h\}}{\mathbb{P}\{z_i = 1, e_i \geq h\}} Y_i - \frac{1}{n} \sum_{i=1}^n \frac{\mathbf{1}\{z_i = 0, e_i \leq 1 - h\}}{\mathbb{P}\{z_i = 0, e_i \leq 1 - h\}} Y_i \quad (3)$$

Our goal then is to select the threshold h in the Horvitz-Thompson estimator that minimizes the MSE. More formally, given a candidate set of thresholds H , we select

$$h^* := \operatorname{argmin}_{h \in H} \operatorname{MSE}(\hat{\tau}_h) = \operatorname{argmin}_{h \in H} \operatorname{Bias}(\hat{\tau}_h)^2 + \operatorname{Var}(\hat{\tau}_h). \quad (4)$$

The intuition here is that for stronger interference, i.e. when $f(e_i)$ is larger for a fixed e_i , the bias introduced by each edge connecting to a neighbor with a different treatment status is higher. The MSE-optimal Horvitz-Thompson estimator in that setting is expected to be one that incorporates a higher exposure threshold. We illustrate this through a display of a bias-variance tradeoff from a noisy linear model $Y_i = \alpha + \beta z_i + \gamma e_i + \epsilon_i$, that occurs across different thresholds for our adaptive Horvitz-Thompson estimator 3 for different ratios of γ/β in the left panel of Figure 1. In the right panel of Figure 1, we illustrate how our approach detects the bias via linear regression for the different γ/β ratios, and together with the exposure distribution, the MSE-optimal threshold (matching the left panel) is selected, represented by the shaded regions.

We refer to this tradeoff as a general one, as due to the dependence structure it is not-necessarily the case where the bias and variance are both monotonically decreasing, and increasing respectively, but the general trend is decreasing and increasing, respectively.

To illustrate how the bias and the variance of the estimator change across different thresholds, we draw upon simple examples from Ugander et al. [2013] in the following subsection. Figure 2 shows the different circulant graphs we consider under unit-level Bernoulli randomization and cluster randomization. We extend this to general graphs in the subsequent sections.

2.1 Tradeoffs in Circulant graphs: Cycles, and k th power Cycle

We first consider unit-level Bernoulli(p) randomization in the cycle graph and the k th-power cycle graphs. We say a graph is a k th power-Cycle graph if there exists an edge between each node and $2k$ of its nearest neighbors Ugander et al. [2013]. We present results for general graphs subsequently.

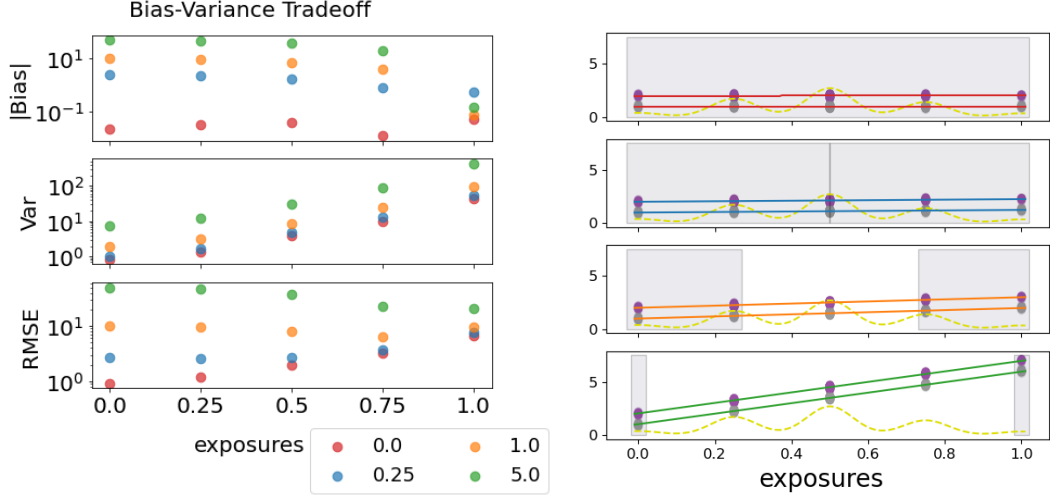


Figure 1: Left: bias, variance, and RMSE of the thresholding Horvitz-Thompson estimator across different thresholds for the 1000-node 2nd-power cycle graph with unit-level randomization, and noisy linear model outcome $Y_i = 10 + 10z_i + \gamma e_i + \epsilon_i$, for $\epsilon_i \sim \mathcal{N}(0, 1)$, γ/β ratios of 0 (red), 0.25 (blue), 1 (orange), and 5 (green). Right: The linear fits (with colors corresponding to the γ/β ratios on the left) is used to approximate the induced exposure bias included by the thresholding. The dotted exposure distribution (yellow) demonstrates the amount of variance reduction by including more data through the thresholding. The rectangular blocks illustrate the regions including the data under the MSE-optimal threshold.

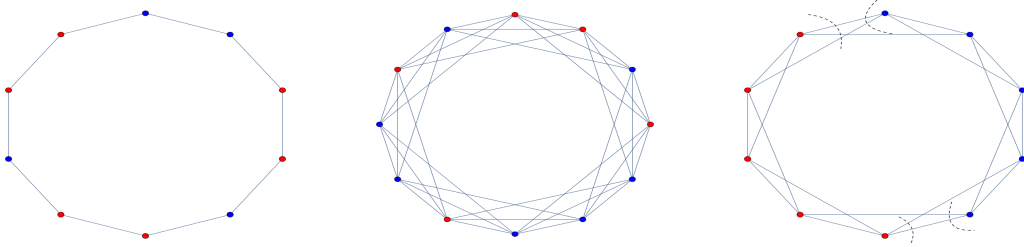


Figure 2: Circulant graphs with unit-level randomization and cluster-level randomization. Blue and red nodes represent treated and control units, respectively. Left: cycle graph with $\text{Ber}(0.5)$ unit randomization. Center: 3rd-power cycle graph with $\text{Bernoulli}(0.5)$ unit randomization. Right: 2nd-power cycle graph with $\text{Bernoulli}(0.5)$ cluster randomization, with clusters of size 5 ($=2k + 1$).

Proposition 1 (Absolute bias in k -th power cycle graphs under unit-randomization). *When $p = 1/2$ and the potential outcome model is simply linear, i.e. $Y_i = \alpha + \beta z_i + \gamma e_i$, the absolute bias of the Horvitz-Thompson estimator for a given threshold $h \equiv l/2k$ for $l = 0, 2, \dots, 2k$, in the k -th-power cycle graph, under unit-level randomization, is equal to $\gamma \times \left[\frac{\sum_{r=l}^{2k} \binom{r/k-1}{r} \binom{2k}{r}}{\sum_{r=l}^{2k} \binom{2k}{r}} - 1 \right]$.*

Proposition 2 (Variance in k -th power cycle graphs under unit-randomization). *When $p = 1/2$ and the potential outcome model is simply linear, i.e. $Y_i = \alpha + \beta z_i + \gamma e_i$, the variance of the Horvitz-Thompson estimator for a given threshold h , in the k -th power cycle graph, under unit-level randomization is proportional to*

$$\mathcal{O} \left(\frac{1}{np^d} [(\alpha + \beta + \gamma dh)^2 + (\alpha + \beta + \gamma d(1-h))^2 - 2\gamma h(1-h)d] \right).$$

Therefore, the optimal threshold h^* depends on γ, β, n, p, d , the graph structure, and the number of other candidate thresholds. In particular, we note the following general regimes:

1. when $\gamma \gg \beta$, then $\text{Bias}(\hat{\tau}_h)^2 \gg \text{Var}(\hat{\tau}_h)$ for large enough n , i.e. $n \gg p^d$. Then, h^* would be higher (closer to one).
2. when $\gamma \ll \beta$, then $\text{Bias}(\hat{\tau}_h)^2 \ll \text{Var}(\hat{\tau}_h)$ for not so large n with fixed d , i.e. $n \approx p^d$, and $\text{Bias}(\hat{\tau}_h)^2 \gg \text{Var}(\hat{\tau}_h)$ for larger n . Therefore, we expect that h^* decreases as the MSE transitions from the former to the latter regime.
3. when $\gamma \approx \beta$, then for some n , we are in the in-between regime, and h^* would be closer to $\frac{1}{2}$. For larger n (while keeping d fixed), the $\text{Bias}(\hat{\tau}_h)^2 \gg \text{Var}(\hat{\tau}_h)$, and we expect to optimally compensate for this by increasing h^* towards 1.

For k th-power cycle graphs, we also consider cluster-randomized design with cluster size $2k + 1$. In Ugander et al. [2013], the authors show that this clustering size minimizes variance under full neighborhood exposure. We state the approximate absolute bias and variance for this setting in the following propositions. Here, define the threshold $h = \frac{l}{d}$ with $l = 0, 1, \dots, d$.

Proposition 3 (Absolute bias in k -th power cycle graph under cluster-randomization). *When $p = 1/2$, and the potential outcome model is simply linear, i.e. $Y_i = \alpha + \beta z_i + \gamma e_i$, the bias of the Horvitz-Thompson estimator for a given threshold h in the k -th power cycle graph under cluster randomization, with cluster-sizes $2k + 1$, is approximately $2\gamma(h - 1)$ for $h \geq 1/2$.*

Proposition 4 (Variance in the k -th power cycle graph under cluster-randomization). *When $p = 1/2$ and the potential outcome model is simply linear, i.e. $Y_i = \alpha + \beta z_i + \gamma e_i$, the variance of the Horvitz-Thompson estimator for a given threshold h , in the k -th power cycle graph under cluster-level randomization, with cluster-sizes $2k + 1$, is proportional to*

$$\frac{1}{np^2} (3d + 1 - 2dh) [(\beta + \gamma h)^2 + (\gamma(1 - h))^2].$$

Under cluster randomization with cluster sizes $2k + 1$ for the k -th power cycle graphs, the variance grows linearly in the degrees of the graph. Therefore, informally, compared to the unit-randomized design setting, higher node degrees lead to stronger bias than variance for a fixed exposure function $f(e_i)$.

3 Estimating the rate of change of bias and variance

In reality, however, one does not have access to the bias and variance. With the goal of thresholding in mind, we obtain a "bias-signal" computed via a linear model, to estimate how the bias incurred changes by including more data under a wider bandwidth corresponding to a smaller threshold h . We propose the following absolute bias-signal estimator:

$$\hat{b}(\hat{\tau}_h) = \frac{1}{n} \sum_{i=1}^n \frac{(1 - e_i) \hat{\gamma} \mathbf{1}\{Z_i = 1, e_i \geq h\}}{\mathbf{P}\{Z_i = 1, e_i \geq h\}} + \frac{1}{n} \sum_{i=1}^n \frac{e_i \hat{\gamma} \mathbf{1}\{Z_i = 0, e_i \leq 1 - h\}}{\mathbf{P}\{Z_i = 0, e_i \leq 1 - h\}},$$

where $\hat{\gamma}$ is the linear regression coefficient of the outcome on the exposure variable.

Therefore, if the dependence of the outcome on the treatment exposure is "strongly positive", $\hat{\gamma}$ would be larger, indicating that including more data with a smaller threshold h would induce more bias than when the dependence on the treatment exposure was "weaker".

Next, to estimate the reduction in the variance for a drop in the threshold h , we estimate the variance of the Horvitz-Thompson estimator at a given threshold h using the variance estimator discussed in Aronow and Samii [2017]. To conserve space, we write this out in Appendix A.1

Since our approach involves "double-dipping" into the data, we need to make sure that there is no overfitting that occurs. The authors of Chernozhukov et al. [2018], Belloni et al. [2015], and Kennedy [2022] describe this in more detail. While sample-splitting would simply take care of this in the case of independent data, we do not have this under the graph dependence structure we are concerned with. We propose to use our approach on the whole sample data and argue this via empirical process theory arguments. In particular, we can think of our threshold h as a nuisance parameter, and we show that our estimator for h has a simple enough associated MSE function class. We note that it is sufficient to show that we are not overfitting too much by showing that the rate of convergence of the estimated MSE under \hat{h} converges to the true MSE under the optimal threshold, under the best possible linear fit, h_{BL}^* at least at a $\mathcal{O}(n^{-1/2})$ -rate.

Proposition 5. *Suppose that Conditions 1, 2, 3, and 4 are satisfied. The corresponding bias terms in the estimated and true MSE, \mathbb{M}_n^b , and M_n^b , under “double prediction”, satisfy*

$$\mathbb{E} \left[\sup_{\delta/2 < |h_{BL}^* - \hat{h}_n| < \delta} \sqrt{n} \left(\mathbb{M}_n^b(\hat{h}_n) - M_n^b(\hat{h}_n) - \mathbb{M}_n^b(h_{BL}^*) - M_n^b(h_{BL}^*) \right) \right] \rightarrow 0,$$

as $\delta \rightarrow 0$.

Indeed, the terms with differences of the linear regression coefficients from the best linear coefficient under a random design on $[0, 1]$ composed with uniformly bounded inverse propensity weights have bounded entropy integral. That is, Donsker conditions are satisfied using Van Der Vaart et al. [1996, Lemma 3.4.3] under Assumptions 1, 2, and 3, 4, and stochastic equicontinuity above holds. We also have marginal Central-Limit theorem with respect to the best linear fit holding for each of the sample-mean-like and U -statistics-like terms in the MSE. Additionally, the latter in the variance parts (see also Chen et al. [2010]) of uniformly bounded inverse propensity weights composed with terms of bounded variation paired with sub-exponential noise (since we have products of sub-gaussians), have bounded entropy integral Van Der Vaart et al. [1996], which then implies a uniform Central Limit Theorem for all of the terms. See Appendix A.5 for a more complete proof.

4 Theoretical and Empirical Results

We now present theoretical and simulation results in the context of general graphs. Our exposure maps depend on respondents’ local neighborhoods, meaning that the only restrictions we need are on the size of those neighborhoods. We discuss an extension to more general exposure maps in the Discussion. Denote by H the set of exposure thresholds we consider. Therefore, in the cycle graphs, $H = \{\frac{u}{d} : u \in \{0, 1, \dots, d\}\}$ where d is the degree of the graph.

4.1 Theory

Condition 1 (Positivity). *For all $i \in [n]$, $r \in \{0, 1\}$,*

$$\mathbb{P}(Z_i = r) > 0$$

Definition 1 (Bounded statistical leverage, Hsu et al. [2012]). *There exists some finite $b > 1$, such that*

$$\frac{\|\Sigma^{-1/2}x\|}{\sqrt{\mathbb{E}[\|\Sigma^{-1/2}x\|^2]}} \equiv \frac{\|\Sigma^{-1/2}x\|}{\sqrt{2}} \leq b.$$

By the positivity assumption 1, bounded statistical leverage holds. More on statistical leverage can be found in Mahoney et al. [2011], Martinsson and Tropp [2020], Young [2019], Pilanci and Wainwright [2015]. The idea, informally, is that for homogeneous statistical leverage across the input data, there are no observations that have too much control over the linear regression.

In our setting larger spread, as well as large enough data near the boundaries $\{0, 1\}$ are important for the robustness to non-linear models. In particular, having more high-leverage data (at the boundaries) allows for our linear fit to be more informative in estimating the bias of the average treatment effect, even in the presence of the non-linearity. That is, our approach is best when we are able to approximate the slope at the boundaries well, regardless of the true potential outcome model.

Condition 2 (Bounded variation treatment-exposure function). *Let the potential outcome function be $y_i = \alpha + \psi(z_i, e_i) + \epsilon_i$ as in 1. The function $\psi(z_i, e_i)$ has bounded variation.*

Definition 2 (Bounded approximation error, Hsu et al. [2012]). *Denote $[\beta_{BL}, \gamma_{BL}]$ by θ , and $[z, e]$ by x . There exists finite $b_{approx} \geq 0$ such that, almost surely,*

$$\frac{\|\Sigma^{-1/2}x(\psi(x) - \langle \theta, x \rangle)\|}{\sqrt{\mathbb{E}[\|\Sigma^{-1/2}x\|^2]}} = \frac{\|\Sigma^{-1/2}x(\psi(x) - \langle \theta, x \rangle)\|}{\sqrt{2}} \leq b_{approx}.$$

That is, together with Condition 1, we assume that there exists finite $b_{approx} \geq 0$, such that $|(f(x) - \langle \theta, x \rangle)| \leq b_{approx}/b$. The following then holds:

$$\begin{aligned} \frac{1}{\sqrt{2}} \|\Sigma^{-1/2}x(\psi(x) - \langle \theta, x \rangle)\| &\leq \frac{1}{\sqrt{2}} \|\Sigma^{-1/2}x\| |\langle \psi(x) - \langle \theta, x \rangle \rangle| \\ &\leq b |\langle \psi(x) - \langle \theta, x \rangle \rangle| \leq b_{approx}. \end{aligned}$$

Condition 3 (Subgaussian noise). *There exists $0 \leq \sigma^2 < \infty$ such that for all $i \in [n]$,*

$$\mathbb{E}[\exp(\lambda(\epsilon_i))] \leq \exp(\lambda^2 \sigma^2 / 2)$$

almost surely for all $\lambda \in \mathbb{R}$.

Condition 4 (Bounded first-order interactions). *Let $B_r(i)$ denote the ball of radius r around unit i . For all $i \in [n]$,*

$$|B_1(i)| = O(1).$$

The condition above is important under unit-randomization design. For a cluster-randomization design, we would require bounded interactions across clusters. In particular the graph interference structure should have small k_n -conductance (i.e. the k_n -partition generalization of the Cheeger constant) for k_n growing with n . Though restrictive theoretically, it is consistent with the observation that networks in practice tend to be sparse and clustered [Chandrasekhar et al., 2020]. Violating this condition will violate exposure positivity (see remark below), and Proposition 5 will not hold.

Remark. In the weighted graph setting, if practitioners consider equivalence classes \tilde{e}_i of exposures, so that $\tilde{e}_i \equiv \tilde{e}_j$ if and only if $|e_i - e_j| < \epsilon_n$ for ϵ_n specified below, exposure positivity, i.e. for all $i \in [n]$, $r \in \{0, 1\}$, and $s \in [0, 1]$, $\mathbf{P}(Z_i = r, \tilde{e}_i = s) > 0$ is satisfied. Then, we can weaken our bounded degree constraint. Let $B_r(i)$ denote the ball of radius r around unit i , such that it decomposes, $|B_1(i)| = |B_1^S(i)| + |B_1^W(i)|$ for all $i \in [n]$. $B_1^S(i)$ is the ball of radius 1 around unit i with strong connections η_{is} , and $|B_1^W(i)|$ be the ball of radius 1 around unit i with weak connections δ_{iw} such that $\sup_{i,s,w} \frac{\eta_{is}}{\delta_{iw}} \rightarrow \infty$. For all $i \in [n]$, we require that $|B_1^S(i)| = O(1)$. With an abuse of notation, write $e_i(\mathcal{N})$ to mean the exposure of unit i as a function of the treated units in the subset $\mathcal{N} \subseteq B_1(i)$. Then, we require also also that $e_i(B_1^S(i)) = \Omega(e_i(B_1(i)))$. Additionally, defining $v_i = z_i - \mathbf{E}[z_i]$ for random variables z_i , $|B_1(i)|$ must satisfy the three conditions in Chandrasekhar et al. [2023] generalizing Aronow and Samii [2017], with an additional condition that the sum of the affinity set covariances is $\Omega(n)$, for the bias terms as well as the variance terms in the MSE. Since those conditions nest strong mixing dependence structure, which nests our current results for the variance terms, these conditions are sufficient. Then, taking $\epsilon_n := \varepsilon(\delta_n, B_1^W(i)) > 0$, gives us uniform control on the estimated MSE of the estimator with respect to the true MSE of the estimator, and all the results follow through.

The circulant graphs we consider are the ring graphs that maintain out-of-synchronization in Wiley et al. [2006]. This points to the sparsity of the circulant graphs. Some examples of graph classes that fall under the categorization of Condition 4 are expander graphs, and growth-restricted graphs Alon [1986], Arora et al. [2009], Gkantsidis et al. [2003], Kuhn et al. [2005], Krauthgamer and Lee [2003], Kowalski [2019]. In the causal inference literature, the effect of the growth-restricted graph setting was studied in Ugander et al. [2013]. For expository purposes, in Section 2.1, we focus our analysis and simulations on a special case of circulant graphs in growth-restricted graphs, particularly the cycle graph, and the k -th power Cycle graphs, just as in Ugander et al. [2013].

Define $M_n(h)$, $M_n(h_{BL}^*)$, $M_n(h^*)$ to be the MSE, evaluated at an arbitrary threshold h , at the optimal threshold under the best possible linear fit, and at the optimal threshold generally, respectively. Then, we have,

$$|M_n(h) - M_n(h^*)| \leq |M_n(h) - M_n(h_{BL}^*)| + |M_n(h_{BL}^*) - M_n(h^*)| \quad (5)$$

$$\leq |M_n(h) - M_n(h_{BL}^*)| + \text{approx}, \quad (6)$$

where

$$\begin{aligned} \text{approx} = & \left| \frac{1}{n} \sum_{i=1}^n \sum_{x_i \in X_i} \{(\mathbf{1}\{x \geq h_{BL}^*\})\gamma_{BL}(1-x) - \mathbf{1}\{x \geq h^*\}(f(1) - f(x))\} \right. \\ & \left. + (\mathbf{1}\{x \leq 1 - h_{BL}^*\})\gamma_{BL}x - \mathbf{1}\{x \leq 1 - h^*\}(f(x) - f(0))\} \right|, \end{aligned}$$

where x_i ranges over the set X_i of possible fractions of unit i 's degree.

How well the linear model approximates the outcome-dependence on the exposure partly describes this quantity. If the potential outcome model does indeed depend linearly on the exposure, this error is identically zero. Additionally, the more spread-out the exposure distribution towards the boundaries $\{0, 1\}$, the better the approximation across $[0, 1-h]$ and $[h, 1]$ both of which characterizes $|h_{BL}^* - h^*|$, and hence the smaller the approximation error. Graph structures that are more sparse for

unit-level randomization, or graph structures with inherent strong clustering such that the edges have high intra-cluster density and much lower inter-cluster density, with growing number of clusters for cluster-randomization, allow for more spread-out exposure distributions. That is, in the latter, under cluster-randomization for graphs with small k_n -conductance for k_n growing with n , we have a more spread-out exposure distribution, as exposure concentration occurs towards more than one centroid depending on the graph clusters formed, with some centroids being at the boundaries as a result of cluster-randomization. See also the note after Condition 4.

In the following theorem, we characterize the probability of choosing the correct threshold under the best linear fit (i.e. the probability the first term on the right-hand-side in 5 is zero).

Theorem 1. *Suppose that $\mathbb{M}_n(h)$ is the estimated MSE, and $M_n(h)$ is the true MSE, associated with a given graph of n nodes and experimental design. Assume that Conditions 1, 2, 3, and 4 hold. Then, define $K := \mathbb{E}[\|\Sigma^{-1/2}x\text{approx}(x)\|^2]$, $\hat{F} := \left(\frac{1}{n} \sum_{i=1}^n \left[\frac{\mathbf{1}_{\{z_i=1, e_i \geq h\}}}{\mathbb{P}\{z_i=1, e_i \geq h\}} e_i + \frac{\mathbf{1}_{\{z_i=0, e_i \leq 1-h\}}}{\mathbb{P}\{z_i=0, e_i \leq 1-h\}} (1 - e_i) \right]^2\right)$, $\Delta := \min_{h, h': h \neq h'} |M_n(h) - M_n(h')|$, $R := \max_i d_i$, and B to be the maximum over $i \in [n]$ of the summands in $\mathbb{M}_n(h)$ and $M_n(h)$, with $Y_i - \epsilon_i$ in the variance terms. $B < \infty$ by Conditions 1, 2, and 4. Let H be the set of candidate thresholds. By Condition 4, $|H| \leq S$ for some constant $S < \infty$. Let γ_0 be the best possible linear fit. Then,*

$$\mathbb{P}\{|M_n(h) - M_n(h_{BL}^*)|\} \geq 1 - 3SC \exp\left(-\frac{n}{C_1(16K^2 + 2\sigma^2)} \cdot \left(\frac{\phi^2 \Delta}{12\gamma_0 \hat{F}} - C_2\right)\right),$$

for some constants C, C_1, C_2 , and variance ϕ^2 of e_i .

This gives us the following corollary.

Corollary 1. *For the k -th-power cycle graph of n nodes, under a noisy linear outcome model, i.e., where $g_0(z_i) = \beta z_i$, and $f_0(e_i) = \gamma_0 e_i$, and $\epsilon_i \sim \mathcal{N}(0, 1)$ for all $i \in [n]$,*

$$\mathbb{P}\{|M_n(h) - M_n(h^*)|\} \geq 1 - 3(2k + 1)C \exp\left(-\frac{n}{C_1(16K^2 + 2\sigma^2)} \cdot \left(\frac{\phi^2 \Delta}{12\gamma_0 \hat{F}} - C_2\right)\right),$$

for some constants C, C_1, C_2 , and variance ϕ^2 of e_i .

4.2 Simulations

We now compare the performance of our approach to that of the Horvitz-Thompson estimator with threshold one, and the Horvitz-Thompson estimator with threshold zero. Additionally, since our objective is essentially an MSE-optimal bandwidth selection problem for the indicator kernel (see Appendix A.3, 13), we compare our estimator to the Horvitz-Thompson estimator with the plugin threshold from Lepski's method Goldenshluger and Lepski [2011], Su et al. [2020]. We note that Lepski's method requires monotonicity of the bias and the variance to work well. In our setting, due to the implicit dependency structure from the graph in the inverse-propensity weights, the monotonicity assumption may be violated (see left panel of Figure 1). We write the three estimators out in Appendix A.2.

In Figure 3, under the linear model with $\alpha = 10$, $g(z_i) = \beta z_i = 10z_i$, $f(e_i) = \gamma e_i$, and $\epsilon_i \sim \mathcal{N}(0, 1)$, we see that our adaptive thresholding estimator (AdaThresh) consistently performs better than existing estimators, "interpolating" between the fixed 0/1-threshold Horvitz-Thompson estimators, and out-performing the Lepski's method plug-in estimators when the threshold γ/β is high.

4.3 Real Data

We evaluate the performance of our estimator on the Amazon (DVD) products similarity network Leskovec et al. [2007]. We consider the performance of the estimator on a subset of (the first) 1000 non-isolated nodes from a total of 19828 nodes, with exposure probabilities computed on the full graph. We generate simulated data using the linear model with $\alpha = 10$, $g(z_i) = \beta z_i = 10z_i$, $f(e_i) = \gamma e_i$, and $\epsilon_i \sim \mathcal{N}(0, 1)$ under a unit-level Bernoulli(0.5) randomization design. Figure 4 shows that we consistently perform better than existing fixed estimators. See Appendix A.7 for more details.

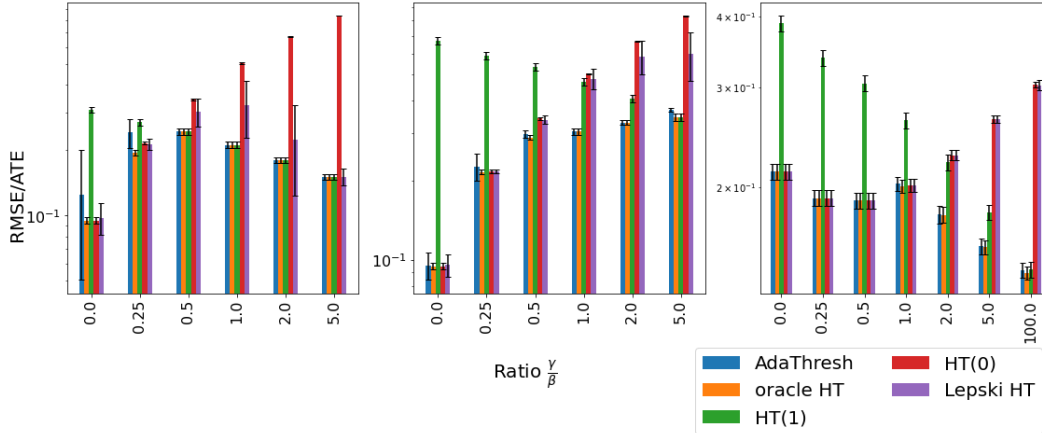


Figure 3: RMSE (normalized by the ATE) induced by the different Horvitz-Thompson estimators. Left: Cycle graph under unit-level $\text{Ber}(0.5)$ randomization. Center: 2nd-power cycle graph under unit-level $\text{Ber}(0.5)$ randomization. Right: 2nd-power cycle graph under cluster-level $\text{Ber}(0.5)$ randomization with cluster sizes 5 ($=2k + 1$). The error bars are two times the standard deviation.

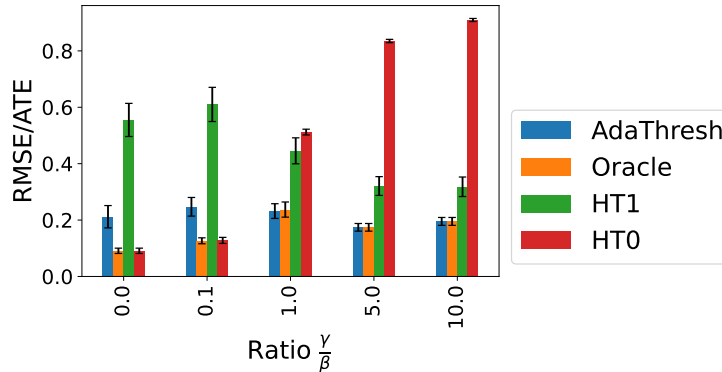


Figure 4: RMSE (normalized by the ATE) across different thresholds on the Amazon product network data. The error bars are two times the standard deviation.

5 Discussion

In this paper, we investigated the adaptive Horvitz-Thompson estimator for symmetric thresholds h and $1 - h$ for treatment and control, respectively. One could also use this approach for a more general estimator with thresholds h_1 and $1 - h_0$, respectively with $h_1 \neq h_0$. Additionally, in Appendix A.7.4, we demonstrate the performance of this approach using the Difference-in-Means estimator incorporating exposure thresholds. In Appendix A.7.3, we illustrate the robustness of our estimator to deviations from linearity in the potential outcomes model. We note that our framework would apply in more general settings, including a direct extension to friends-of-friends (or further connections) or to neighborhoods that are either observed or learned through a clustering algorithm. An additional interesting future direction could be to explore an extension of our work to the framework presented in Chandrasekhar et al. [2023], which allows each individual to have a unique exposure and then bins exposures that are separated by at least a threshold.

Furthermore, to improve upon robustness to non-linear settings, we propose an extension using local regression to estimate the rate of change of bias within the $[0, 1 - h]$, $[h, 1]$ windows. As long as there is sufficient concentration of exposures in these windows, robustness is never worse. In Appendix A.7.5, we display our simulation results in this setting using local linear regression to estimate the rate of change of bias within the $[0, 1 - h]$, $[h, 1]$ windows. One could also use other local regression approaches, such as kernel regression, etc., while maintaining sufficiently small model complexity to avoid needing to sample-split.

Acknowledgments and Disclosure of Funding

The authors would like to thank Alex Kokot, and Lars van der Laan for helpful discussions; and Matthew Eichhorn for suggesting the Amazon product similarity network dataset.

References

- Damon Centola and Michael Macy. Complex Contagions and the Weakness of Long Ties. *American Journal of Sociology*, 113(3):702–734, 2007.
- Daron Acemoglu, Asuman Ozdaglar, and Ercan Yildiz. Diffusion of innovations in social networks. In *2011 50th IEEE conference on decision and control and European control conference*, pages 2329–2334. IEEE, 2011.
- Bryony Reich. The diffusion of innovations in social networks. *Working paper, University College London*, 2016.
- Peter M Aronow and Cyrus Samii. Estimating average causal effects under general interference, with application to a social network experiment. 2017.
- Johan Ugander, Brian Karrer, Lars Backstrom, and Jon Kleinberg. Graph cluster randomization: Network exposure to multiple universes. In *Proceedings of the 19th ACM SIGKDD international conference on Knowledge discovery and data mining*, pages 329–337, 2013.
- Daniel L Sussman and Edoardo M Airoidi. Elements of estimation theory for causal effects in the presence of network interference. *arXiv preprint arXiv:1702.03578*, 2017.
- Morgan Hardy, Rachel M Heath, Wesley Lee, and Tyler H McCormick. Estimating spillovers using imprecisely measured networks. *arXiv preprint arXiv:1904.00136*, 2019.
- Eric Auerbach and Max Tabord-Meehan. The local approach to causal inference under network interference. *arXiv preprint arXiv:2105.03810*, 2021.
- Dean Eckles, Brian Karrer, and Johan Ugander. Design and analysis of experiments in networks: Reducing bias from interference. *Journal of Causal Inference*, 5(1):20150021, 2017.
- Panos Toulis and Edward Kao. Estimation of causal peer influence effects. In *International conference on machine learning*, pages 1489–1497. PMLR, 2013.
- Guillaume W Basse and Edoardo M Airoidi. Model-assisted design of experiments in the presence of network-correlated outcomes. *Biometrika*, 105(4):849–858, 2018.
- Jing Cai, Alain De Janvry, and Elisabeth Sadoulet. Social networks and the decision to insure. *American Economic Journal: Applied Economics*, 7(2):81–108, 2015.
- Hongtao Zhu, Sizhe Zhang, Yang Su, Zhenyu Zhao, and Nan Chen. Integrating active learning in causal inference with interference: A novel approach in online experiments. *arXiv preprint arXiv:2402.12710*, 2024.
- Yi Su, Pavithra Srinath, and Akshay Krishnamurthy. Adaptive estimator selection for off-policy evaluation. In *International Conference on Machine Learning*, pages 9196–9205. PMLR, 2020.
- Jianqing Fan and Irene Gijbels. Variable bandwidth and local linear regression smoothers. *The Annals of Statistics*, pages 2008–2036, 1992.
- David Ruppert. Empirical-bias bandwidths for local polynomial nonparametric regression and density estimation. *Journal of the American Statistical Association*, 92(439):1049–1062, 1997.
- Nathan Kallus and Angela Zhou. Policy evaluation and optimization with continuous treatments. In *International conference on artificial intelligence and statistics*, pages 1243–1251. PMLR, 2018.
- Alexander Goldenshluger and Oleg Lepski. Bandwidth selection in kernel density estimation: oracle inequalities and adaptive minimax optimality. 2011.
- Alexandre Belloni, Fei Fang, and Alexander Volfovsky. Neighborhood adaptive estimators for causal inference under network interference. *arXiv preprint arXiv:2212.03683*, 2022.

- Victor Chernozhukov, Denis Chetverikov, Mert Demirer, Esther Duflo, Christian Hansen, Whitney Newey, and James Robins. Double/debiased machine learning for treatment and structural parameters. *The Econometrics Journal*, 21(1):C1–C68, 01 2018. ISSN 1368-4221. doi: 10.1111/ectj.12097. URL <https://doi.org/10.1111/ectj.12097>.
- Alexandre Belloni, Victor Chernozhukov, Ivan Fernández-Val, and Christian Hansen. Program evaluation with high-dimensional data. Technical report, cemmap working paper, 2015.
- Edward H Kennedy. Semiparametric doubly robust targeted double machine learning: a review. *arXiv preprint arXiv:2203.06469*, 2022.
- Aad W Van Der Vaart, Jon A Wellner, Aad W van der Vaart, and Jon A Wellner. *Weak convergence*. Springer, 1996.
- Louis HY Chen, Larry Goldstein, and Qi-Man Shao. *Normal approximation by Stein's method*. Springer Science & Business Media, 2010.
- Daniel Hsu, Sham M Kakade, and Tong Zhang. Random design analysis of ridge regression. In *Conference on learning theory*, pages 9–1. JMLR Workshop and Conference Proceedings, 2012.
- Michael W Mahoney et al. Randomized algorithms for matrices and data. *Foundations and Trends® in Machine Learning*, 3(2):123–224, 2011.
- Per-Gunnar Martinsson and Joel A Tropp. Randomized numerical linear algebra: Foundations and algorithms. *Acta Numerica*, 29:403–572, 2020.
- Alwyn Young. Channeling fisher: Randomization tests and the statistical insignificance of seemingly significant experimental results. *The quarterly journal of economics*, 134(2):557–598, 2019.
- Mert Pilanci and Martin J Wainwright. Randomized sketches of convex programs with sharp guarantees. *IEEE Transactions on Information Theory*, 61(9):5096–5115, 2015.
- Arun G Chandrasekhar, Horacio Larreguy, and Juan Pablo Xandri. Testing models of social learning on networks: Evidence from two experiments. *Econometrica*, 88(1):1–32, 2020.
- Arun G Chandrasekhar, Matthew O Jackson, Tyler H McCormick, and Vydhourie Thiyageswaran. General covariance-based conditions for central limit theorems with dependent triangular arrays. *arXiv preprint arXiv:2308.12506*, 2023.
- Daniel A Wiley, Steven H Strogatz, and Michelle Girvan. The size of the sync basin. *Chaos: An Interdisciplinary Journal of Nonlinear Science*, 16(1), 2006.
- Noga Alon. Eigenvalues, geometric expanders, sorting in rounds, and ramsey theory. *Combinatorica*, 6(3): 207–219, 1986.
- Sanjeev Arora, Satish Rao, and Umesh Vazirani. Expander flows, geometric embeddings and graph partitioning. *Journal of the ACM (JACM)*, 56(2):1–37, 2009.
- Christos Gkantsidis, Milena Mihail, and Amin Saberi. Conductance and congestion in power law graphs. In *Proceedings of the 2003 ACM SIGMETRICS International Conference on Measurement and modeling of computer systems*, pages 148–159, 2003.
- Fabian Kuhn, Thomas Moscibroda, and Rogert Wattenhofer. On the locality of bounded growth. In *Proceedings of the twenty-fourth annual ACM symposium on Principles of distributed computing*, pages 60–68, 2005.
- Robert Krauthgamer and James R Lee. The intrinsic dimensionality of graphs. In *Proceedings of the thirty-fifth annual ACM symposium on Theory of computing*, pages 438–447, 2003.
- Emmanuel Kowalski. *An introduction to expander graphs*. Société mathématique de France Paris, 2019.
- Jure Leskovec, Lada A Adamic, and Bernardo A Huberman. The dynamics of viral marketing. *ACM Transactions on the Web (TWEB)*, 1(1):5–es, 2007.
- Aad W Van der Vaart. *Asymptotic statistics*, volume 3. Cambridge university press, 2000.
- Alessio Sancetta. Maximal inequalities for u-processes of strongly mixing random variables. *Probability and Mathematical Statistics*, 29, 2009.
- Eric Beutner and Henryk Zähle. Deriving the asymptotic distribution of u-and v-statistics of dependent data using weighted empirical processes. 2012.

Ken-ichi Yoshihara. Limiting behavior of u-statistics for stationary, absolutely regular processes. *Zeitschrift für Wahrscheinlichkeitstheorie und verwandte Gebiete*, 35(3):237–252, 1976.

Miguel Angel Arcones and Bin Yu. Central limit theorems for empirical and u-processes of stationary mixing sequences. *Journal of Theoretical Probability*, 7(1):47–71, 1994.

Manfred Denker and Gerhard Keller. Rigorous statistical procedures for data from dynamical systems. *Journal of Statistical Physics*, 44:67–93, 1986.

Sourav Chatterjee. *Concentration inequalities with exchangeable pairs*. Stanford University, 2005.

A Appendix / supplemental material

A.1 Variance estimator

The variance estimator, for the Horvitz-Thompson estimator, we use is the one proposed by Aronow and Samii [2017, Eqn. 7,9].

$$\begin{aligned}
\widehat{Var}(\hat{\tau}_h) &= \sum_{i=1}^n \frac{\mathbf{1}\{z_i = 1, e_i \geq h\} Y_i^2}{n^2 \pi_i^1} \left(\frac{1}{\pi_i^1} - 1 \right) \\
&+ \sum_{i=1}^n \sum_{\substack{j=1 \\ j \neq i}}^n \frac{\mathbf{1}\{z_i = 1, e_i \geq h\} \mathbf{1}\{z_j = 1, e_j \geq h\} Y_i Y_j}{n^2 \pi_{ij}^{11}} \left(\frac{\pi_{ij}^{11}}{\pi_i^1 \pi_j^1} - 1 \right) \\
&+ \sum_{i=1}^n \frac{\mathbf{1}\{z_i = 0, e_i \leq 1 - h\} Y_i^2}{n^2 \pi_i^0} \left(\frac{1}{\pi_i^0} - 1 \right) \\
&+ \sum_{i=1}^n \sum_{\substack{j=1 \\ j \neq i}}^n \frac{\mathbf{1}\{z_i = 0, e_i \leq 1 - h\} \mathbf{1}\{z_j = 0, e_j \leq 1 - h\} Y_i Y_j}{n^2 \pi_{ij}^{00}} \left(\frac{\pi_{ij}^{00}}{\pi_i^0 \pi_j^0} - 1 \right) \\
&- \frac{2}{n^2} \sum_{i=1}^n \sum_{j \in [n]; \pi_{ij}^{10} > 0} (\mathbf{1}\{z_i = 1, e_i \geq h\} \mathbf{1}\{z_j = 0, e_j \leq 1 - h\} Y_i Y_j) \left(\frac{1}{\pi_i^1 \pi_j^0} - \frac{1}{\pi_{ij}^{10}} \right) \\
&+ \frac{2}{n^2} \sum_{i=1}^n \sum_{j \in [n]; \pi_{ij}^{10} = 0} \left(\frac{\mathbf{1}\{z_i = 1, e_i \geq h\} Y_i^2}{2\pi_i^1} + \frac{\mathbf{1}\{z_j = 0, e_j \leq 1 - h\} Y_j^2}{2\pi_j^0} \right)
\end{aligned} \tag{7}$$

Here, π_i^x, π_{ij}^{xy} are defined with respect to the threshold h . That is, $\pi_i^1 = \mathbb{P}\{z_i = 1, e_i \geq h\}$, $\pi_i^0 = \mathbb{P}\{z_i = 0, e_i \leq 1 - h\}$, $\pi_{ij}^{10} = \mathbb{P}\{z_i = 1, e_i \geq h, z_j = 0, e_j \leq 1 - h\}$, $\pi_{ij}^{11} = \mathbb{P}\{z_i = 1, e_i \geq h, z_j = 1, e_j \geq h\}$, $\pi_{ij}^{01} = \mathbb{P}\{z_i = 0, e_i \leq 1 - h, z_j = 1, e_j \geq h\}$, $\pi_{ij}^{00} = \mathbb{P}\{z_i = 0, e_i \leq 1 - h, z_j = 0, e_j \leq 1 - h\}$.

A.2 Horvitz-Thompson estimators with existing approaches

We write the vanilla Horvitz-Thompson estimator (at threshold one) 8, the Horvitz-Thompson estimator at threshold zero 9, and the Horvitz-Thompson estimator with the threshold selected via Lepski's method 12 below.

A.2.1 Vanilla Horvitz-Thompson estimator (at threshold one)

$$\hat{\tau}_{HT1} = \frac{1}{n} \sum_{i=1}^n \frac{\mathbf{P}\{Z_i = 1, e_i = 1\}}{\mathbf{1}\{Z_i = 1, e_i = 1\}} Y_i - \frac{1}{n} \sum_{i=1}^n \frac{\mathbf{1}\{Z_i = 0, e_i = 0\}}{\mathbf{P}\{Z_i = 0, e_i = 0\}} Y_i \tag{8}$$

A.2.2 Horvitz-Thompson estimator at threshold zero

$$\hat{\tau}_{HT0} = \frac{1}{n} \sum_{i=1}^n \frac{\mathbf{P}\{Z_i = 1\}}{\mathbf{1}\{Z_i = 1\}} Y_i - \frac{1}{n} \sum_{i=1}^n \frac{\mathbf{1}\{Z_i = 0\}}{\mathbf{P}\{Z_i = 0\}} Y_i \tag{9}$$

A.2.3 Lepski's method

As described in Su et al. [2020], we first take

$$I(h) := [\hat{\tau}_{\text{HT}_h} - 2\hat{\text{SDE}}\text{V}(\hat{\tau}_{\text{HT}_h}), \hat{\tau}_{\text{HT}_h} + 2\hat{\text{SDE}}\text{V}(\hat{\tau}_{\text{HT}_h})]. \quad (10)$$

Then, take

$$\hat{h}_{\text{Lepski}} := \min\{h \in H : \cap_{h=1}^k I(h) \neq \emptyset\}, \quad (11)$$

and

$$\hat{\tau}_{\text{LepskiHT}} = \frac{1}{n} \sum_{i=1}^n \frac{\mathbf{1}\{Z_i = 1, e_i \geq \hat{h}_{\text{Lepski}}\}}{\mathbf{P}\{Z_i = 1, e_i \geq \hat{h}_{\text{Lepski}}\}} Y_i - \frac{1}{n} \sum_{i=1}^n \frac{\mathbf{1}\{Z_i = 0, e_i \leq 1 - \hat{h}_{\text{Lepski}}\}}{\mathbf{P}\{Z_i = 0, e_i \leq 1 - \hat{h}_{\text{Lepski}}\}} Y_i \quad (12)$$

A.3 An equivalent formulation of the Horvitz-Thompson estimator for exposure threshold h

We can rewrite the display in 3 in the following form:

$$\hat{\tau}_h = \frac{1}{n} \sum_{i=1}^n \frac{\mathbf{1}\{|z_i - e_i| \leq h\}}{\mathbb{P}\{|z_i - e_i| \leq h\}} \tilde{z}_i Y_i \quad (13)$$

where $\tilde{z}_i = 2z_i - 1$, so that $\tilde{z}_i \in \{-1, 1\}$. It is then clear that the threshold h controls how much dissimilarity between the treatment status of units and their neighbors, we allow in our estimation. This allows us to reframe the problem as an optimal bandwidth selection one.

A.4 Proofs to Propositions 1, 2, 3, 4

Proof to Proposition 1. When $p = 1/2$ and the potential outcome model is simply linear, i.e. $Y_i = \alpha + \beta z_i + \gamma e_i$, the absolute bias of the Horvitz-Thompson estimator for a given threshold $h \equiv l/2k$ for $l = 0, 2, \dots, 2k$, in the k th-power cycle graph under unit-randomization is equal to is equal to

$$\begin{aligned} & \frac{1}{\mathbb{P}\{z_i = 1, e_i \geq h\}} \sum_{x_i \in X} \mathbf{1}\{x_i \geq h\} \mathbb{E}[\mathbf{1}\{z_i = 1, e_i = x_i\}] y_i(x_i) \\ & - \frac{1}{\mathbb{P}\{z_i = 0, e_i \leq 1 - h\}} \sum_{x_i \in X} \mathbf{1}\{x_i \leq 1 - h\} \mathbb{E}[\mathbf{1}\{z_i = 0, e_i = x_i\}] y_i(x_i) \\ & - (\beta + \gamma) \\ & = \frac{1}{\sum_{r=l}^{2k} \binom{2k}{r} p^{2k}} \sum_{x_i \in X} \mathbf{1}\{x_i \geq h\} \mathbb{E}[\mathbf{1}\{z_i = 1, e_i = x_i\}] y_i(x_i) \\ & - \frac{1}{\sum_{r=l}^{2k} \binom{2k}{r} p^{2k}} \sum_{x_i \in X} \mathbf{1}\{x_i \leq 1 - h\} \mathbb{E}[\mathbf{1}\{z_i = 0, e_i = x_i\}] y_i(x_i) \\ & - (\beta + \gamma) \\ & = \frac{p^{2k}}{\sum_{r=l}^{2k} \binom{2k}{r} p^{2k}} \left(\sum_{r=l}^{2k} \binom{2k}{r} \beta + \binom{2k}{r} (r/k - 1) \gamma \right) - (\beta + \gamma) \\ & = \frac{1}{\sum_{r=l}^{2k} \binom{2k}{r} p^{2k}} \left(\sum_{r=l}^{2k} \binom{2k}{r} (r/k - 1) \gamma \right) - \gamma \end{aligned}$$

where $X = \{0, 1/2k, 2/2k, \dots, 1\}$. □

Proof to Proposition 2. When $p = 1/2$ and the potential outcome model is simply linear, i.e. $Y_i = \alpha + \beta z_i + \gamma e_i$, it is not difficult to see that the variance of the Horvitz-Thompson estimator for a given threshold $h \equiv l/2k$, in the k -th power cycle graph under unit-level randomization is proportional to

$$\begin{aligned} & \frac{1}{n} \sum_{l=0}^{2k} \binom{2k}{l} \mathbf{1}\{l/2k \geq h\} \left[(\alpha + \beta + \gamma l/2k)^2 \left(\frac{1}{\sum_{l=0}^{2k} \binom{2k}{l} \mathbf{1}\{l/2k \geq h\} p^{2k}} - 1 \right) \right. \\ & \quad \left. + 2(\beta + \gamma l/(2k))(\gamma(1 - l/2k))(2k + 1 - \frac{2k}{\sum_{l=0}^{2k} \binom{2k}{l} \mathbf{1}\{l/2k \geq h\} p^{2k}}) \right. \\ & \quad \left. + (\alpha + \gamma(1 - l/2k))^2 \left(\frac{1}{\sum_{l=0}^{2k} \binom{2k}{l} \mathbf{1}\{l/2k \geq h\} p^{2k}} - 1 \right) \right]. \end{aligned}$$

Considering the dominating terms gives us the result. □

Proof to Proposition 3. When $p = 1/2$ and the potential outcome model is simply linear, i.e. $Y_i = \alpha + \beta z_i + \gamma e_i$, the absolute bias of the Horvitz-Thompson estimator for a given threshold $h \equiv l/2k$ for $l = k, k + 1, \dots, 2k$, in the k th-power cycle graph under cluster-randomization is equal to is equal to

$$\begin{aligned}
& \frac{1}{\mathbb{P}\{z_i = 1, e_i \geq h\}} \sum_{x_i \in X} \mathbf{1}\{x_i \geq h\} \mathbb{E}[\mathbf{1}\{z_i = 1, e_i = x_i\}] y_i(x_i) \\
& - \frac{1}{\mathbb{P}\{z_i = 0, e_i \leq 1 - h\}} \sum_{x_i \in X} \mathbf{1}\{x_i \leq 1 - h\} \mathbb{E}[\mathbf{1}\{z_i = 0, e_i = x_i\}] y_i(x_i) \\
& - (\beta + \gamma) \\
& = \frac{(p/(2k+1) + 2k/(2k+1) \cdot p^2)(\beta + \gamma) + 2p/(2k+1) \sum_{r=1}^k \mathbf{1}\{r \geq d-l\}(\beta + \gamma \cdot (2l-d)/d)}{p/(2k+1) + p^2 \cdot 2k/(2k+1) + 2p/(2k+1) \sum_{r=1}^k \mathbf{1}\{r \geq d-l\}} \\
& - (\beta + \gamma) \\
& = \mathcal{O}(2\gamma(h-2))
\end{aligned}$$

where $X = \{0, 1/2k, 2/2k, \dots, 1\}$. When $l < k$, the bias scales is the same as when $l = k$. \square

Proof to Proposition 4. When $p = 1/2$ and the potential outcome model is simply linear, i.e. $Y_i = \alpha + \beta z_i + \gamma e_i$, it is not difficult to see that the variance of the Horvitz-Thompson estimator for a given threshold $h \equiv l/2k$, in the k -th power cycle graph under cluster-randomization, with cluster-size $2k + 1$, is proportional to

$$\begin{aligned}
& \sum_{u=0}^d \mathbf{1}\{u/d \geq h\} \binom{d}{u} \sum_{i=1}^n \left(\frac{(\beta + \gamma u/d)^2}{n^2} \right) [(3d+1-2l) \left(\frac{1}{p^2} - 1 \right) + (2l+1) \left(\frac{1}{p} - 1 \right)] \\
& + \sum_{u=0}^d \mathbf{1}\{u/d \geq h\} \binom{d}{u} \sum_{i=1}^n \left(\frac{(\gamma \frac{d-u}{d})^2}{n^2} \right) [(3d+1-2l) \left(\frac{1}{p^2} - 1 \right) + (2l+1) \left(\frac{1}{p} - 1 \right)] \\
& - \sum_{u=0}^d \mathbf{1}\{u/d \geq h\} \binom{d}{u} \frac{2}{n} (\beta + \gamma \cdot u/d) (\gamma \cdot \frac{d-u}{d}).
\end{aligned}$$

Considering the dominating terms gives us the result. \square

A.5 Proof to Proposition 5

Suppose that Conditions 1, 2, 3, and 4 are satisfied. We aim to show that the corresponding biases in the MSE terms under “double prediction” satisfy

$$\mathbb{E} \left[\sup_{\delta/2 < |h_{BL}^* - h_n| < \delta} \sqrt{n} \left(\mathbb{M}_n^b(h_n) - M_n^b(h_n) - \mathbb{M}_n^b(h_{BL}^*) - M_n^b(h_{BL}^*) \right) \right] \rightarrow 0,$$

as $\delta \rightarrow 0$, where x_i ranges over the set X_i of possible fractions of degree i .

Proof. We begin by considering the empirical process in question. We write out

$$\begin{aligned}
\mathbb{M}_n(h) &= \left(\frac{1}{n} \sum_{i=1}^n \frac{\hat{\gamma}_h(1 - e_i) \mathbf{1}\{Z_i = 1, e_i \geq h\}}{\mathbf{P}\{Z_i = 1, e_i \geq h\}} + \frac{1}{n} \sum_{i=1}^n \frac{\hat{\gamma}_h(1 - e_i) \mathbf{1}\{Z_i = 1, e_i \geq h\}}{\mathbf{P}\{Z_i = 1, e_i \geq h\}} \right)^2 \\
&+ \sum_{i=1}^n \frac{\mathbf{1}\{z_i = 1, e_i \geq h\} Y_i^2}{n^2 \pi_i^1} \left(\frac{1}{\pi_i^1} - 1 \right) \\
&+ \sum_{i=1}^n \sum_{\substack{j=1 \\ j \neq i}}^n \frac{\mathbf{1}\{z_i = 1, e_i \geq h\} \mathbf{1}\{z_j = 1, e_j \geq h\} Y_i Y_j}{n^2 \pi_{ij}^{11}} \left(\frac{\pi_{ij}^{11}}{\pi_i^1 \pi_j^1} - 1 \right) \\
&+ \sum_{i=1}^n \frac{\mathbf{1}\{z_i = 0, e_i \leq 1 - h\} Y_i^2}{n^2 \pi_i^0} \left(\frac{1}{\pi_i^0} - 1 \right) \\
&+ \sum_{i=1}^n \sum_{\substack{j=1 \\ j \neq i}}^n \frac{\mathbf{1}\{z_i = 0, e_i \leq 1 - h\} \mathbf{1}\{z_j = 0, e_j \leq 1 - h\} Y_i Y_j}{n^2 \pi_{ij}^{00}} \left(\frac{\pi_{ij}^{00}}{\pi_i^0 \pi_j^0} - 1 \right) \\
&- \frac{2}{n^2} \sum_{i=1}^n \sum_{j \in [n]; \pi_{ij}^{10} > 0} (\mathbf{1}\{z_i = 1, e_i \geq h\} \mathbf{1}\{z_j = 0, e_j \leq 1 - h\} Y_i Y_j) \left(\frac{1}{\pi_i^1 \pi_j^0} - \frac{1}{\pi_{ij}^{10}} \right) \\
&+ \frac{2}{n^2} \sum_{i=1}^n \sum_{j \in [n]; \pi_{ij}^{10} = 0} \left(\frac{\mathbf{1}\{z_i = 1, e_i \geq h\} Y_i^2}{2\pi_i^1} + \frac{\mathbf{1}\{z_j = 0, e_j \leq 1 - h\} Y_j^2}{2\pi_j^0} \right).
\end{aligned}$$

The absolute Horvitz-Thompson bias estimate at threshold h (and $1 - h$) is

$$\hat{b}(h) = \frac{1}{n} \sum_{i=1}^n \frac{\hat{\gamma}(1 - e_i) \mathbf{1}\{Z_i = 1, e_i \geq h\}}{\mathbf{P}(Z_i = 1, e_i \geq h)} + \frac{1}{n} \sum_{i=1}^n \frac{\hat{\gamma}(e_i) \mathbf{1}\{Z_i = 0, e_i \leq 1 - h\}}{\mathbf{P}(Z_i = 0, e_i \leq 1 - h)} \quad (14)$$

The true-bias is

$$\begin{aligned}
b^*(h) &= \frac{1}{n} \sum_{i=1}^n \sum_{x_i \in X_i} \mathbf{1}\{x_i \geq h\} y_i(1, x_i) - \frac{1}{n} \sum_{i=1}^n \sum_{x_i \in X_i} \mathbf{1}\{Z_i = 0, e_i \leq 1 - h\} y_i(0, x_i) \\
&- \frac{1}{n} \sum_{i=1}^n y_i(1, 1) + \frac{1}{n} \sum_{i=1}^n y_i(0, 0),
\end{aligned}$$

where x_i ranges over the set X_i of possible fractions of degree i ,

Then, for every h , using the identity $x^2 - y^2 = (x + y)(x - y)$, we have

$$\mathbb{M}_n^b(h) - M_n^b(h) \leq 3b^*(h) \left(\hat{b}(h) - b^*(h) \right)$$

We can decompose the second term on the right-hand-side above into the true bias induced by the best possible linear fit, and the residual true bias:

$$\hat{b}(h) - b^*(h) = (\hat{b}(h) - b_{BL}^*(h)) + (b_{BL}^*(h) - b^*(h))$$

where

$$\begin{aligned}
\hat{b}(h) - b_{BL}^*(h) &= \left(\frac{1}{n} \sum_{i=1}^n \frac{\hat{\gamma} \mathbf{1}\{Z_i = 1, e_i \geq h\}}{\mathbf{P}(Z_i = 1, e_i \geq h)} - \left(\frac{1}{n} \sum_{i=1}^n y_i^{BL}(1, 1) - \frac{1}{n} \sum_{i=1}^n y_i^{BL}(0, 0) \right) \right) \\
&- \left(\frac{1}{n} \sum_{i=1}^n \frac{\hat{\gamma} e_i \mathbf{1}\{Z_i = 1, e_i \geq h\}}{\mathbf{P}(Z_i = 1, e_i \geq h)} - \frac{1}{n} \sum_{i=1}^n \sum_{x_i \in X_i} \mathbf{1}\{x_i \geq h\} y_i^{BL}(x_i) \right) \\
&+ \left(\frac{1}{n} \sum_{i=1}^n \frac{\hat{\gamma} e_i \mathbf{1}\{Z_i = 0, e_i \leq 1 - h\}}{\mathbf{P}(Z_i = 0, e_i \leq 1 - h)} - \frac{1}{n} \sum_{i=1}^n \sum_{x_i \in X_i} \mathbf{1}\{x_i \leq 1 - h\} y_i^{BL}(x_i) \right),
\end{aligned}$$

where y_i^{BL} is the projection of y_i onto the best possible linear fit. Next,

$$\begin{aligned}
b_{BL}^*(h) - b^*(h) &= \left(\frac{1}{n} \sum_{i=1}^n y_i^{BL}(1, 1) - \frac{1}{n} \sum_{i=1}^n y_i(1, 1) \right) \\
&\quad - \left(\frac{1}{n} \sum_{i=1}^n \sum_{x_i \in X_i} \mathbf{1}\{x_i \geq h\} y_i^{BL}(x_i) - \frac{1}{n} \sum_{i=1}^n \frac{\mathbf{1}\{Z_i = 1, e_i \geq h\}}{\mathbf{P}\{Z_i = 1, e_i \geq h\}} Y_i \right) \\
&\quad + \left(\frac{1}{n} \sum_{i=1}^n \sum_{x_i \in X_i} \mathbf{1}\{x_i \leq 1 - h\} y_i^{BL}(x_i) - \frac{1}{n} \sum_{i=1}^n \frac{\mathbf{1}\{Z_i = 0, e_i \leq 1 - h\}}{\mathbf{P}\{Z_i = 0, e_i \leq 1 - h\}} Y_i \right) \\
&\quad - \left(\frac{1}{n} \sum_{i=1}^n y_i^{BL}(0, 0) - \frac{1}{n} \sum_{i=1}^n y_i(0, 0) \right).
\end{aligned}$$

We first consider the terms in $b_{BL}^*(h) - b^*(h)$. By Conditions 4, 2, 3, each of these terms are sample-means of sub-gaussians corresponding to the approximation error induced by a linear fit, with bounded dependency.

We now proceed to consider each of the terms in $\hat{b}(h) - b_{BL}^*(h)$ above. Each of the three parentheses satisfy Donsker conditions. Indeed, under Conditions 1, 2, 3, and 4, they are sample-mean terms with uniformly bounded coefficients, and $\hat{\gamma}$ converges at a rate of $\mathcal{O}(n^{-1/2})$, which we compose with $3b^*(h)$ (see Section 3.4.3.2. in Van Der Vaart et al. [1996]). Thus, the terms in $\mathbb{M}_n^b(h) - M_n^b(h)$ have bounded entropy integral. Under our bounded-variation potential-outcome model (Condition 2), we have that $\log N_{[]}(\epsilon, \Theta_n^b, L_2(\mathbf{P})) \leq K(\frac{1}{\epsilon})$, which gives us $\tilde{J}(\delta, \Theta_n^b, L_2(\mathbf{P})) \leq \delta^{1/2}$ Van Der Vaart et al. [1996] (see also Example 19.11 in Van der Vaart [2000]).

Therefore, putting these together, we have the following maximal inequality for the bias terms

$$\mathbb{E} \left[\sup_{\delta/2 < |h_{BL}^* - \hat{h}_n| < \delta} \sqrt{n} \left(\mathbb{M}_n^b(h_n) - M_n^b(h_n) - (\mathbb{M}_n^b(h_{BL}^*) - M_n^b(h_{BL}^*)) \right) \right] \quad (15)$$

$$\leq \tilde{J}(\delta, \Theta_n^b, L_2(\mathbf{P})) \left(1 + \frac{\tilde{J}(\delta, \Theta_n^b, L_2(\mathbf{P}))}{\delta \sqrt{n}} \right), \quad (16)$$

with $\tilde{J}(\delta, \Theta_n^b, L_2(\mathbf{P})) \leq \delta^{1/2}$. Additionally, in the following we consider the variance parts of the MSE terms. The variance estimator we use following Aronow and Samii [2017] is

$$\begin{aligned}
\hat{v}(h) &= \sum_{i=1}^n \frac{\mathbf{1}\{z_i = 1, e_i \geq h\} Y_i^2}{n^2 \pi_i^1} \left(\frac{1}{\pi_i^1} - 1 \right) \\
&\quad + \sum_{i=1}^n \sum_{\substack{j=1 \\ j \neq i}}^n \frac{\mathbf{1}\{z_i = 1, e_i \geq h\} \mathbf{1}\{z_j = 1, e_j \geq h\} Y_i Y_j}{n^2 \pi_{ij}^{11}} \left(\frac{\pi_{ij}^{11}}{\pi_i^1 \pi_j^1} - 1 \right) \\
&\quad + \sum_{i=1}^n \frac{\mathbf{1}\{z_i = 0, e_i \leq 1 - h\} Y_i^2}{n^2 \pi_i^0} \left(\frac{1}{\pi_i^0} - 1 \right) \\
&\quad + \sum_{i=1}^n \sum_{\substack{j=1 \\ j \neq i}}^n \frac{\mathbf{1}\{z_i = 0, e_i \leq 1 - h\} \mathbf{1}\{z_j = 0, e_j \leq 1 - h\} Y_i Y_j}{n^2 \pi_{ij}^{00}} \left(\frac{\pi_{ij}^{00}}{\pi_i^0 \pi_j^0} - 1 \right) \\
&\quad - \frac{2}{n^2} \sum_{i=1}^n \sum_{j \in [n]; \pi_{ij}^{10} > 0} (\mathbf{1}\{z_i = 1, e_i \geq h\} \mathbf{1}\{z_j = 0, e_j \leq 1 - h\} Y_i Y_j) \left(\frac{1}{\pi_i^1 \pi_j^0} - \frac{1}{\pi_{ij}^{10}} \right) \\
&\quad + \frac{2}{n^2} \sum_{i=1}^n \sum_{j \in [n]; \pi_{ij}^{10} = 0} \left(\frac{\mathbf{1}\{z_i = 1, e_i \geq h\} Y_i^2}{2\pi_i^1} + \frac{\mathbf{1}\{z_j = 0, e_j \leq 1 - h\} Y_j^2}{2\pi_j^0} \right).
\end{aligned}$$

The true variance is

$$\begin{aligned}
v^*(h) &= \sum_{i=1}^n \frac{y_i(h^+)^2}{n^2} \left(\frac{1}{\pi_i^1} - 1 \right) \\
&+ \sum_{i=1}^n \sum_{\substack{j=1 \\ j \neq i}}^n \frac{y_i(h^+) y_j(h^+)}{n^2} \left(\frac{\pi_{ij}^{11}}{\pi_i^1 \pi_j^1} - 1 \right) \\
&+ \sum_{i=1}^n \frac{y_i(h^-)^2}{n^2 \pi_i^0} \left(\frac{1}{\pi_i^0} - 1 \right) \\
&+ \sum_{i=1}^n \sum_{\substack{j=1 \\ j \neq i}}^n \frac{y_i(h^-) y_j(h^-)}{n^2} \left(\frac{\pi_{ij}^{00}}{\pi_i^0 \pi_j^0} - 1 \right) \\
&- \frac{2}{n^2} \sum_{i=1}^n \sum_{j \in [n]; \pi_{ij}^{10} > 0} y_i(h^+) y_j(h^-) \left(\frac{\pi_{ij}^{10}}{\pi_i^1 \pi_j^0} - 1 \right) \\
&+ \frac{2}{n^2} \sum_{i=1}^n \sum_{j \in [n]; \pi_{ij}^{10} = 0} y_i(h^+)^2 y_j(h^-)^2.
\end{aligned}$$

Then, we have that

$$\begin{aligned}
\sup_h \hat{v}(h) - v^*(h) &= \sup_h \left[\left(\sum_{i=1}^n \frac{\mathbf{1}\{z_i = 1, e_i \geq h\} Y_i^2}{n^2 \pi_i^1} \left(\frac{1}{\pi_i^1} - 1 \right) - \sum_{i=1}^n \frac{y_i(h^+)^2}{n^2} \left(\frac{1}{\pi_i^1} - 1 \right) \right) \right. \\
&+ \left(\sum_{i=1}^n \sum_{\substack{j=1 \\ j \neq i}}^n \frac{\mathbf{1}\{z_i = 1, e_i \geq h\} \mathbf{1}\{z_j = 1, e_j \geq h\} Y_i Y_j}{n^2 \pi_{ij}^{11}} \left(\frac{\pi_{ij}^{11}}{\pi_i^1 \pi_j^1} - 1 \right) \right. \\
&- \left. \left. \sum_{i=1}^n \sum_{\substack{j=1 \\ j \neq i}}^n \frac{y_i(h^+) y_j(h^+)}{n^2} \left(\frac{\pi_{ij}^{11}}{\pi_i^1 \pi_j^1} - 1 \right) \right) \right. \\
&+ \left(\sum_{i=1}^n \frac{\mathbf{1}\{z_i = 0, e_i \leq 1 - h\} Y_i^2}{n^2 \pi_i^0} \left(\frac{1}{\pi_i^0} - 1 \right) - \sum_{i=1}^n \frac{y_i(h^-)^2}{n^2 \pi_i^0} \left(\frac{1}{\pi_i^0} - 1 \right) \right) \\
&+ \left(\sum_{i=1}^n \sum_{\substack{j=1 \\ j \neq i}}^n \frac{\mathbf{1}\{z_i = 0, e_i \leq 1 - h\} \mathbf{1}\{z_j = 0, e_j \leq 1 - h\} Y_i Y_j}{n^2 \pi_{ij}^{00}} \left(\frac{\pi_{ij}^{00}}{\pi_i^0 \pi_j^0} - 1 \right) \right. \\
&- \left. \left. \sum_{i=1}^n \sum_{\substack{j=1 \\ j \neq i}}^n \frac{y_i(h^-) y_j(h^-)}{n^2} \left(\frac{\pi_{ij}^{00}}{\pi_i^0 \pi_j^0} - 1 \right) \right) \right. \\
&- \left(\frac{2}{n^2} \sum_{i=1}^n \sum_{j \in [n]; \pi_{ij}^{10} > 0} (\mathbf{1}\{z_i = 1, e_i \geq h\} \mathbf{1}\{z_j = 0, e_j \leq 1 - h\} Y_i Y_j) \left(\frac{1}{\pi_i^1 \pi_j^0} - \frac{1}{\pi_{ij}^{10}} \right) \right. \\
&+ \left. \left. \frac{2}{n^2} \sum_{i=1}^n \sum_{j \in [n]; \pi_{ij}^{10} > 0} y_i(h^+) y_j(h^-) \left(\frac{\pi_{ij}^{10}}{\pi_i^1 \pi_j^0} - 1 \right) \right) \right. \\
&+ \left(\frac{2}{n^2} \sum_{i=1}^n \sum_{j \in [n]; \pi_{ij}^{10} = 0} \left(\frac{\mathbf{1}\{z_i = 1, e_i \geq h\} Y_i^2}{2\pi_i^1} + \frac{\mathbf{1}\{z_j = 0, e_j \leq 1 - h\} Y_j^2}{2\pi_j^0} \right) \right. \\
&- \left. \left. \frac{2}{n^2} \sum_{i=1}^n \sum_{j \in [n]; \pi_{ij}^{10} = 0} y_i(h^+)^2 y_j(h^-)^2 \right) \right].
\end{aligned}$$

We consider each of the parentheses above. The first and third terms are both $o(n^{-1/2})$ since the $\frac{\mathbf{1}\{\cdot\}}{\mathbf{P}\{\cdot\}}$ terms in the summands are uniformly bounded. The second, fourth, and fifth terms are V-statistics terms. Together with the centering terms from $M_n(h)$, from Sancetta [2009], Beutner and Zähle [2012], Yoshihara [1976], Arcones and Yu [1994] and Denker and Keller [1986], we see that under bounded (up to fourth) moments, they have uniform $\mathcal{O}(n^{-1/2})$ convergence rates (see also Chen et al. [2010, Theorems 9.1, 9.2]). Finally, we consider the sixth term, and notice that this is $o(n^{-1})$, as there are a bounded number of terms j , under Condition 4, for which $\pi_{ij} = 0$ for each i . Additionally, the smaller the difference between a fully treated outcome and a fully control outcome, i.e. the smaller the range of the outcome, the smaller this term is.

Similar to the bias calculations, under Condition 4, the conditions of Sancetta [2009, Theorem 2.1], have been met, and hence, we have the following maximal inequality from the variance terms:

$$\mathbb{E} \left[\sup_{\delta/2 < |h_{BL} - \hat{h}_n| < \delta} \sqrt{n} (\mathbb{M}_n^v(h_n) - M_n^v(h_n) - (\mathbb{M}_n^v(h_{BL}^*) - M_n^v(h_{BL}^*))) \right] \quad (17)$$

$$\leq \tilde{J}(\delta, \Theta_n^v, L_2(\mathbf{P})) \left(1 + \frac{\tilde{J}(\delta, \Theta_n^v, L_2(\mathbf{P}))}{\delta \sqrt{n}} \right), \quad (18)$$

with $\tilde{J}(\delta, \Theta_n^v, L_2(\mathbf{P})) \leq \delta^{1/2}$.

Therefore, by a triangle inequality, the following stochastic equicontinuity result holds:

$$\mathbb{E} \left[\sup_{\delta/2 < |h_{BL} - \hat{h}_n| < \delta} \sqrt{n} (\mathbb{M}_n(h_n) - M_n(h_n) - (\mathbb{M}_n(h_{BL}^*) - M_n(h_{BL}^*))) \right] \rightarrow 0, \quad (19)$$

as $\delta \rightarrow 0$. \square

A.6 Proof of Theorem 1

Proof. Defining $K := \mathbb{E}[\|\Sigma^{-1/2} x \text{approx}(x)\|^2]$, $\hat{F} := \left(\frac{1}{n} \sum_{i=1}^n \left[\frac{\mathbf{1}\{z_i=1, e_i \geq h\}}{\mathbf{P}\{z_i=1, e_i \geq h\}} e_i + \frac{\mathbf{1}\{z_i=0, e_i \leq 1-h\}}{\mathbf{P}\{z_i=0, e_i \leq 1-h\}} (1 - e_i) \right] \right)^2$, $\Delta := \min_{h, h': h \neq h'} |M_n(h) - M_n(h')|$, $R = \max_i \deg_i$, and B the maximum over $i \in [n]$ of the summands in $\mathbb{M}_n(h)$ and $M_n(h)$ with $Y_i - \epsilon_i$ in the variance terms. Note that $B < \infty$ by Condition 4, and 2. For any $\delta > 0$:

$$\begin{aligned} & \mathbb{P}\{|M_n(h) - M_n(h^*)| \geq \delta\} \\ & \leq \mathbb{P}\{\max_h |\mathbb{M}_n(h, \hat{\gamma}) - M_n(h, \gamma_0)| \geq \frac{\Delta}{2}\} \\ & \leq \sum_{h \in H} \mathbb{P}\{|\mathbb{M}_n(h, \hat{\gamma}) - \mathbb{M}_n(h, \gamma_0) + \mathbb{M}_n(h, \gamma_0) - M_n(h, \gamma_0)| \geq \frac{\Delta}{2}\} \\ & \leq S \left(\mathbb{P}\{|\mathbb{M}_n(h, \hat{\gamma}) - \mathbb{M}_n(h, \gamma_0)| \geq \frac{\Delta}{4}\} + \mathbb{P}\{|\mathbb{M}_n(h, \gamma_0) - M_n(h, \gamma_0)| \geq \frac{\Delta}{4}\} \right) \\ & = S \left(\mathbb{P}\{|\hat{\delta}^2(h, \hat{\gamma}) - \hat{b}^2(h, \gamma_0)| \geq \frac{\Delta}{4}\} + \mathbb{P}\{|\mathbb{M}_n(h, \gamma_0) - M_n(h, \gamma_0)| \geq \frac{\Delta}{4}\} \right) \\ & \leq S \left(\mathbb{P}\{|\hat{\gamma} - \gamma_0| \geq \frac{\Delta}{12\gamma_0 \hat{F}}\} + \mathbb{P}\{|\mathbb{M}_n(h, \gamma_0) - M_n(h, \gamma_0)| \geq \frac{\Delta}{4}\} \right) \\ & \leq S \left(3 \exp \left(-\frac{n}{C_1(16K^2 + 2\sigma^2)} \cdot \left(\frac{\phi^2 \Delta}{12\gamma_0 \hat{F}} - C_2 \right) \right) + \mathbb{P}\{|\mathbb{M}_n(h, \gamma_0) - M_n(h, \gamma_0)| \geq \frac{\Delta}{4}\} \right), \end{aligned}$$

where ϕ^2 is the variance of e_i . The last inequality is obtained from Hsu et al. [2012, Theorem 11], via a simple change of variable argument.

Let M_n^f and \mathbb{M}_n^f denote the true and estimated mean-squared errors with variances involving the de-noised version of Y_i , and M_n^ϵ and \mathbb{M}_n^ϵ denote the remaining terms in the true and estimated mean-squared errors with variances involving only the ϵ_i parts. By a combinatorial Bernstein's inequality Chatterjee [2005], since we have bounded degree (dependence) by R ,

$$\begin{aligned} & \mathbb{P}\{|\mathbb{M}_n(h, \gamma_0) - M_n(h, \gamma_0)| \geq \frac{\Delta}{4}\} \\ & \leq \mathbb{P}\{|\mathbb{M}_n^f(h, \gamma_0) - M_n^f(h, \gamma_0)| \geq \frac{\Delta}{16}\} + \mathbb{P}\{|\mathbb{M}_n^\epsilon(h, \gamma_0) - M_n^\epsilon(h, \gamma_0)| \geq \frac{\Delta}{16}\} \\ & \leq \exp \left(-\frac{\Delta^2}{16^2 (12RB^2 + 4\sqrt{2}B\Delta/16)} \right) + \mathbb{P}\{|\mathbb{M}_n^\epsilon(h, \gamma_0) - M_n^\epsilon(h, \gamma_0)| \geq \frac{\Delta}{16}\} \end{aligned}$$

where the first inequality is obtained via the crude upper-bound $(a + b)^2 \leq 2a^2 + 2b^2$, followed by a union-bound. Finally, we upper-bound the second term on the RHS above using the usual Bernstein inequality. When $\Delta/16 \in [0, \sqrt{2}\sigma^2]$, we have that

$$\mathbb{P}\{|M_n^\epsilon(h, \gamma_0) - M_n^\epsilon(h, \gamma_0)| \geq \frac{\Delta}{16}\} \leq \exp\left(-\frac{n^2\Delta^2}{c16^2 \cdot 2\sigma^4}\right),$$

and when $\Delta/16 > \sqrt{2}\sigma^2$, we have that

$$\mathbb{P}\{|M_n^\epsilon(h, \gamma_0) - M_n^\epsilon(h, \gamma_0)| \geq \frac{\Delta}{16}\} \leq \exp\left(-\frac{n\Delta}{c32 \cdot \sigma^2}\right),$$

Therefore, the dominant terms are the sub-exponential decay terms, giving us that for any $\delta > 0$,

$$\mathbb{P}\{|M_n(h) - M_n(h^*)| \geq \delta\} \leq 3SC \exp\left(-\frac{n}{C_1(16K^2 + 2\sigma^2)} \cdot \left(\frac{\phi^2\Delta}{12\gamma_0\hat{F}} - C_2\right)\right),$$

for some constant C . □

To prove Corollary 1, we note that for k th power cycle graphs, $|H| = 2k + 1$. Additionally, under the linear model, $h^* = h_{BL}^*$.

A.7 Simulations

A.7.1 Experimental details on the Amazon product similarity graph data

The simulations were run on a CPU. Our experiments focus on a subset of the 19828-node DVD graph. In particular, we considered the 17924-node subgraph by removing all isolated nodes. To compute the exposure probabilities, we used 10^6 simulations. We then selected the first 1000 nodes of the 19828 to analyze. 200 replicates were run, generating random treatment assignments and the corresponding outcomes. For each of the replicates, 1000 separate simulation runs were generated to compute the oracle MSEs. In total, this took approximately 2 hours. The graph data is available at: <https://snap.stanford.edu/data/amazon-meta.html>

A.7.2 Experimental details on simulated graphs

All synthetic graph simulations were run on a machine of Intel® Xeon® processors with 48 CPU cores, and 50GB of RAM. We simulated 1000 replicates, generating random treatment assignments and the corresponding outcomes, with each oracle MSE computed using 1000 separate simulation runs. The exposure probabilities under each threshold were computed as proposed in Aronow and Samii [2017] using 1000 simulation iterations. In total, this took approximately 30 minutes on average (across the different potential outcomes, and graph settings). The code is available at: <https://anonymous.4open.science/t/AdaThresh-DDEE/>

A.7.3 Simulations for non-linear potential outcomes models

We investigate the robustness of our estimator to potential outcomes models that are non-linear in the exposure. In particular, we consider simulations from the sigmoid, and sine exposure functions. In Figure 5, we display the performance of our estimator under a sigmoid (left) and sine (right) interference function, respectively. Our adaptive threshold Horvitz-Thompson estimator (AdaThresh) improves upon other existing Horvitz-Thompson estimators.

A.7.4 Simulations for Difference-in-Means estimator with adaptive exposure thresholds

We consider our approach using the Difference-in-Means estimator incorporating exposure thresholds:

$$\hat{\tau}_{\text{DiM}_h} = \frac{\sum_{i=1}^n \mathbf{1}\{Z_i = 1, e_i \geq h\} Y_i}{\sum_{i=1}^n \mathbf{1}\{Z_i = 1, e_i \geq h\}} - \frac{\sum_{i=1}^n \mathbf{1}\{Z_i = 0, e_i \leq 1 - h\} Y_i}{\sum_{i=1}^n \mathbf{1}\{Z_i = 0, e_i \leq 1 - h\}}. \quad (20)$$

We use the following bias estimator:

$$\hat{b}(\hat{\tau}_h) = \sum_{i=1}^n \frac{(1 - e_i)\hat{\gamma}\mathbf{1}\{Z_i = 1, e_i \geq h\}}{\sum_{i=1}^n \mathbf{1}\{Z_i = 1, e_i \geq h\}} + \sum_{i=1}^n \frac{e_i\hat{\gamma}\mathbf{1}\{Z_i = 0, e_i \leq 1 - h\}}{\sum_{i=1}^n \mathbf{1}\{Z_i = 0, e_i \leq 1 - h\}},$$

where $\hat{\gamma}$ is the linear regression coefficient for the exposure variable.

We use the following variance estimator:

$$\hat{V}ar(\hat{\tau}) = \frac{2}{n-1} \left(\hat{V}ar_T + \hat{V}ar_C \right)$$

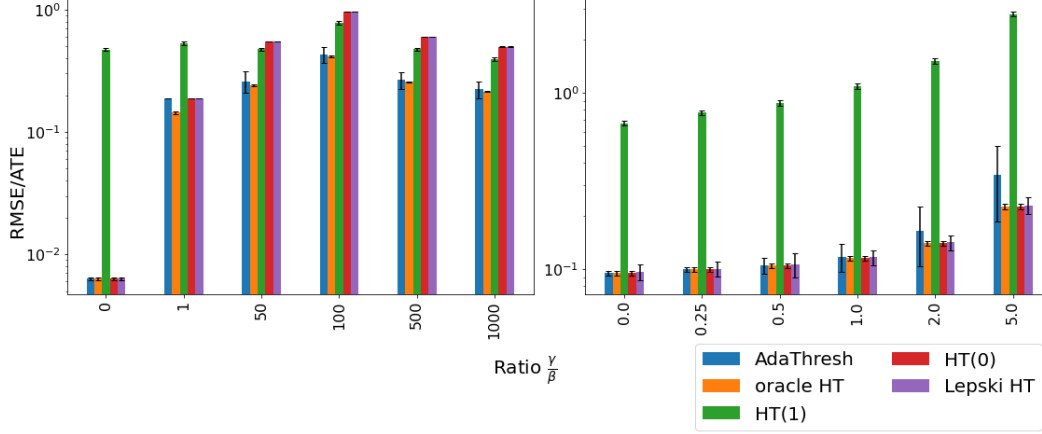


Figure 5: RMSE (normalized by the ATE) induced by the different Horvitz-Thompson estimators. Left: 2nd-power cycle graph under unit-level Ber(0.5) randomization under sigmoid $f(e_i) = \gamma / (1 + \exp(-e_i))$. Right: 2nd-power cycle graph under unit-level Ber(0.5) randomization with $f(e_i) = \gamma(1 - \sin(\pi \cdot e_i))$ being a sine function. The error bars are two times the standard deviation.

where

$$\hat{Var}_T = \frac{1}{n_1} \sum_{i=1}^n \left(Y_i \mathbf{1}\{Z_i = 1, e_i \geq h\} - \frac{1}{n_1} \sum_{i=1}^n Y_i \mathbf{1}\{Z_i = 1, e_i \geq h\} \right)^2$$

where $n_1 := \sum_{i=1}^n \mathbf{1}\{Z_i = 1, e_i \geq h\}$, and

$$\hat{Var}_C = \frac{1}{n_0} \sum_{i=1}^n \left(Y_i \mathbf{1}\{Z_i = 0, e_i \leq 1 - h\} - \frac{1}{n_0} \sum_{i=1}^n Y_i \mathbf{1}\{Z_i = 0, e_i \leq 1 - h\} \right)^2$$

where $n_0 := \sum_{i=1}^n \mathbf{1}\{Z_i = 0, e_i \leq 1 - h\}$.

We compare the performance of our adaptive estimator to the vanilla difference-in-means estimator, the difference-in-means analogue of the vanilla Horvitz-Thompson estimator, and the difference-in-means estimator with a threshold plugin via Lepski's method. We write these out below:

- vanilla difference-in-means estimator

$$\hat{\tau}_{\text{DiM}_0} = \frac{\sum_{i=1}^n \mathbf{1}\{Z_i = 1\} Y_i}{\sum_{i=1}^n \mathbf{1}\{Z_i = 1\}} - \frac{\sum_{i=1}^n \mathbf{1}\{Z_i = 0\} Y_i}{\sum_{i=1}^n \mathbf{1}\{Z_i = 0\}} \quad (21)$$

- difference-in-means estimator at threshold $h = 1$

$$\hat{\tau}_{\text{DiM}_1} = \frac{\sum_{i=1}^n \mathbf{1}\{Z_i = 1, e_i = 1\} Y_i}{\sum_{i=1}^n \mathbf{1}\{Z_i = 1, e_i = 1\}} - \frac{\sum_{i=1}^n \mathbf{1}\{Z_i = 0, e_i = 0\} Y_i}{\sum_{i=1}^n \mathbf{1}\{Z_i = 0, e_i = 0\}} \quad (22)$$

- difference-in-means estimator at threshold \hat{h}_{Lepski} where

$$\hat{h}_{\text{Lepski}} := \min\{h \in H : \cap_{h=1}^k I(h) \neq \emptyset\}, \quad (23)$$

with

$$I(h) := [\hat{\tau}_{\text{DiM}_h} - 2\text{SD}\hat{\text{EV}}(\hat{\tau}_{\text{DiM}_h}), \hat{\tau}_{\text{DiM}_h} + 2\text{SD}\hat{\text{EV}}(\hat{\tau}_{\text{DiM}_h})], \quad (24)$$

and

$$\hat{\tau}_{\text{LepskiDiM}} = \sum_{i=1}^n \frac{\mathbf{1}\{Z_i = 1, e_i \geq \hat{h}_{\text{Lepski}}\}}{\sum_{i=1}^n \mathbf{1}\{Z_i = 1, e_i \geq \hat{h}_{\text{Lepski}}\}} Y_i - \sum_{i=1}^n \frac{\mathbf{1}\{Z_i = 0, e_i \leq 1 - \hat{h}_{\text{Lepski}}\}}{\sum_{i=1}^n \mathbf{1}\{Z_i = 0, e_i \leq 1 - \hat{h}_{\text{Lepski}}\}} Y_i \quad (25)$$

In Figures 6 and 7, we display the performance of our adaptive threshold (AdaThresh) Difference-in-Means estimators in comparison to other estimators. AdaThresh improves upon fixed threshold Difference-in-Means estimators.

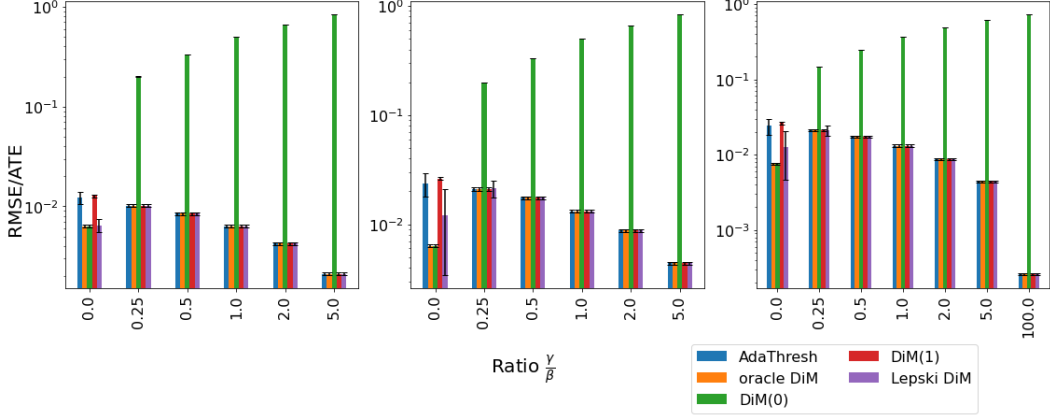


Figure 6: RMSE (normalized by the ATE) under the linear model with $\alpha = 10$, $g(z_i) = \beta z_i = 10z_i$, $f_0(e_i) = \gamma e_i$, and $\epsilon_i \sim \mathcal{N}(0, 1)$, induced by the different Difference-in-Means estimators. Left: Cycle graph under unit-level $\text{Ber}(0.5)$ randomization. Center: 2nd-power cycle graph under unit-level $\text{Ber}(0.5)$ randomization. Right: 2nd-power cycle graph under cluster-level $\text{Ber}(0.5)$ randomization with cluster sizes 5 ($=2k + 1$). The error bars are two times the standard deviation.

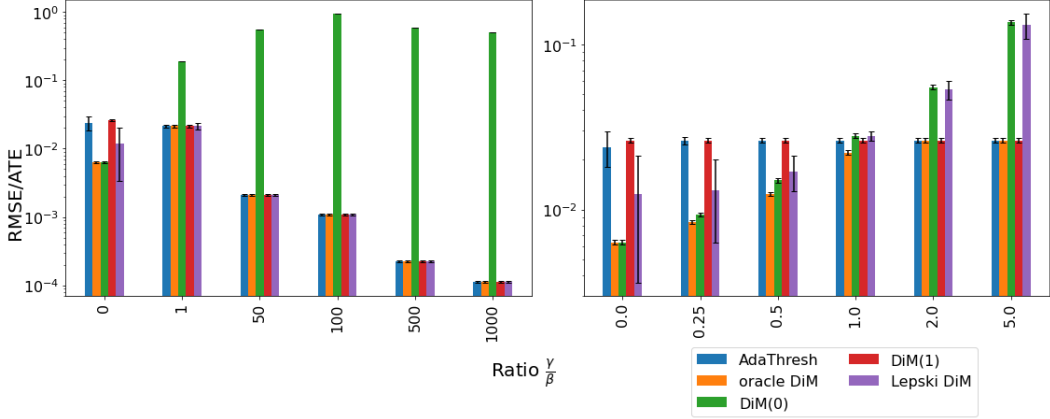


Figure 7: RMSE (normalized by the ATE) induced by the different Difference-in-Means estimators. Left: 2nd-power cycle graph under unit-level $\text{Ber}(0.5)$ randomization under sigmoid $f(e_i) = \gamma/(1 + \exp(-e_i))$. Right: 2nd-power cycle graph under unit-level $\text{Ber}(0.5)$ randomization with $f(e_i) = \gamma(1 - \sin(\pi \cdot e_i))$ being a sine function. The error bars are two times the standard deviation.

A.7.5 Simulations using local linear regression

We extend our global linear regression approach to a local linear regression one to estimate the rate of change of the bias. We write the new bias estimators for the Horvitz-Thompson and Difference-in-Means estimators. We illustrate the performance of the local linear regression in the settings above, as well as settings that significantly deviates from linearity.

We write the bias estimator for the Horvitz-Thompson estimator as:

$$\hat{b}(\hat{\tau}_h) = \frac{1}{n} \sum_{i=1}^n \frac{(1 - e_i) \hat{\gamma}_h \mathbf{1}\{Z_i = 1, e_i \geq h\}}{\mathbf{P}\{Z_i = 1, e_i \geq h\}} + \frac{1}{n} \sum_{i=1}^n \frac{e_i \hat{\gamma}_{1-h} \mathbf{1}\{Z_i = 0, e_i \leq 1 - h\}}{\mathbf{P}\{Z_i = 0, e_i \leq 1 - h\}},$$

where $\hat{\gamma}_h$ and $\hat{\gamma}_{1-h}$ are the local linear regression coefficients for the exposure variable in the intervals $[h, 1]$, and $[0, 1 - h]$, respectively.

Similarly, write the bias estimator for the Difference-in-Means estimator as:

$$\hat{b}(\hat{\tau}_h) = \sum_{i=1}^n \frac{(1 - e_i) \hat{\gamma}_h \mathbf{1}\{Z_i = 1, e_i \geq h\}}{\sum_{i=1}^n \mathbf{1}\{Z_i = 1, e_i \geq h\}} + \sum_{i=1}^n \frac{e_i \hat{\gamma}_{1-h} \mathbf{1}\{Z_i = 0, e_i \leq 1 - h\}}{\sum_{i=1}^n \mathbf{1}\{Z_i = 0, e_i \leq 1 - h\}},$$

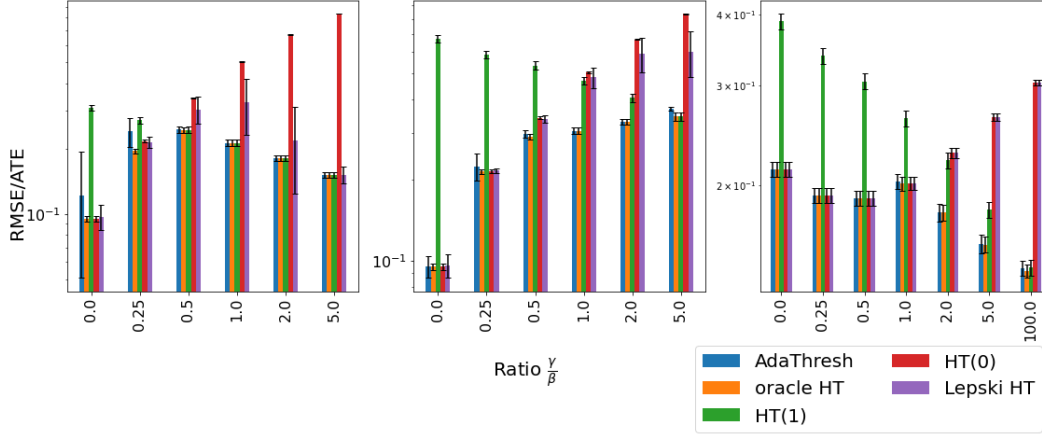


Figure 8: RMSE (normalized by the ATE) under the linear model with $\alpha = 10$, $g(z_i) = \beta z_i = 10z_i$, $f(e_i) = \gamma e_i$, and $\epsilon_i \sim \mathcal{N}(0, 1)$, induced by the different (local) Horvitz-Thompson estimators. Left: Cycle graph under unit-level $\text{Ber}(0.5)$ randomization. Center: 2nd-power cycle graph under unit-level $\text{Ber}(0.5)$ randomization. Right: 2nd-power cycle graph under cluster-level $\text{Ber}(0.5)$ randomization with cluster sizes 5 ($=2k + 1$). The error bars are two times the standard deviation.

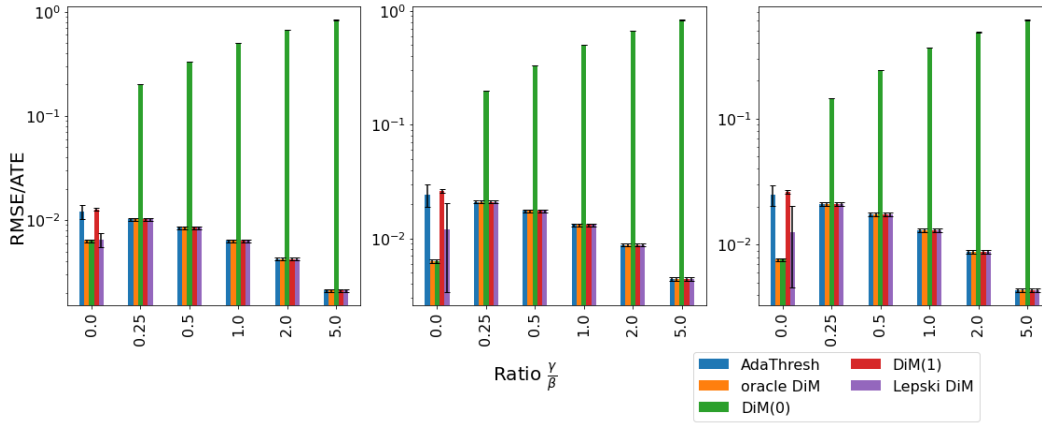


Figure 9: RMSE (normalized by the ATE) under the linear model with $\alpha = 10$, $g(z_i) = \beta z_i = 10z_i$, $f(e_i) = \gamma e_i$, and $\epsilon_i \sim \mathcal{N}(0, 1)$, induced by the different (local) Difference-in-Means estimators. Left: Cycle graph under unit-level $\text{Ber}(0.5)$ randomization. Center: 2nd-power cycle graph under unit-level $\text{Ber}(0.5)$ randomization. Right: 2nd-power cycle graph under cluster-level $\text{Ber}(0.5)$ randomization with cluster sizes 5 ($=2k + 1$). The error bars are two times the standard deviation.

where $\hat{\gamma}_h$ and $\hat{\gamma}_{1-h}$ are the local linear regression coefficients for the exposure variable in the intervals $[h, 1]$, and $[0, 1 - h]$, respectively.

Figures 8, 10, 9, and 11, display how local linear regression bias estimates perform.

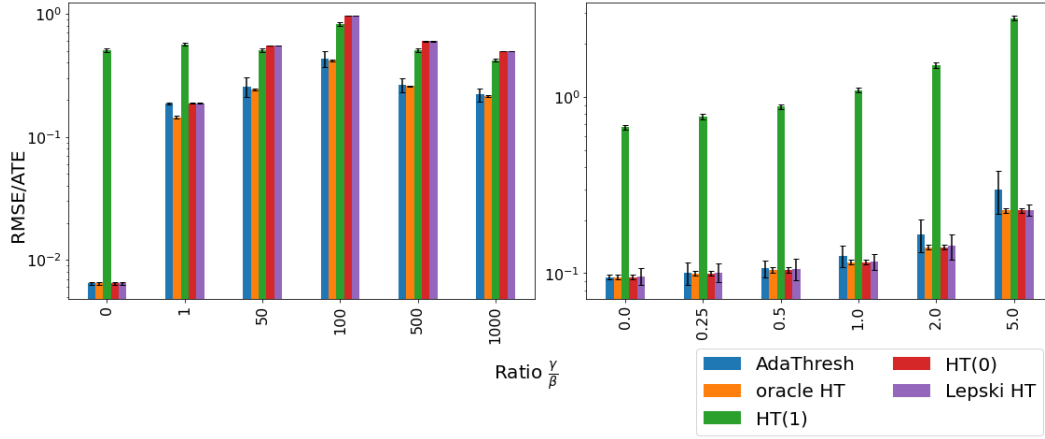


Figure 10: RMSE (normalized by the ATE) under the linear model with $\alpha = 10$, $g(z_i) = \beta z_i = 10z_i$, $\epsilon_i \sim \mathcal{N}(0, 1)$, induced by the different (local) Horvitz-Thompson estimators. Left: 2nd-power cycle graph under unit-level Ber(0.5) randomization under sigmoid $f(e_i) = \gamma/(1 + \exp(-e_i))$. Right: 2nd-power cycle graph under unit-level Ber(0.5) randomization with $f(e_i) = \gamma(1 - \sin(\pi \cdot e_i))$ being a sine function. The error bars are two times the standard deviation.

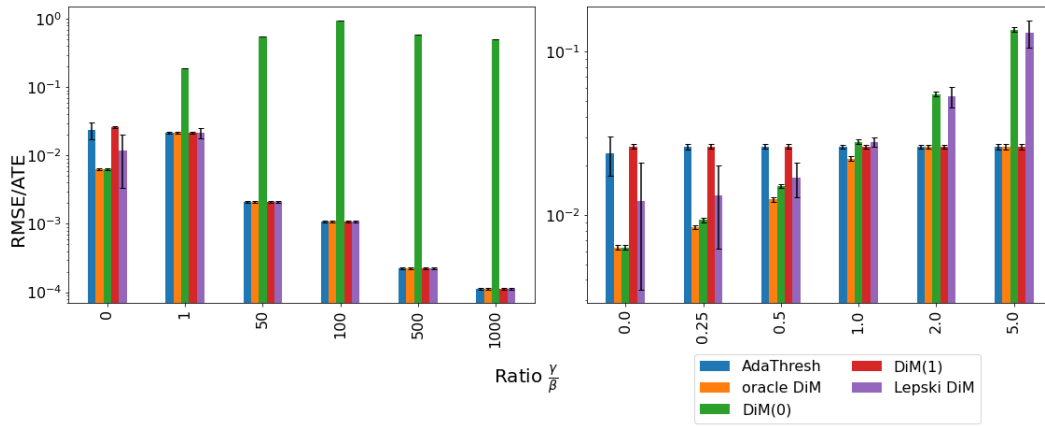


Figure 11: RMSE (normalized by the ATE) induced by the different (local) Difference-in-Means estimators. Left: 2nd-power cycle graph under unit-level Ber(0.5) randomization under sigmoid $f(e_i) = \gamma/(1 + \exp(-e_i))$. Right: 2nd-power cycle graph under unit-level Ber(0.5) randomization with $f(e_i) = \gamma(1 - \sin(\pi \cdot e_i))$ being a sine function. The error bars are two times the standard deviation.